Review article

The snowball Earth hypothesis: testing the limits of global change

Paul F. Hoffman* and Daniel P. Schrag

Department of Earth and Planetary Sciences, Harvard University, Cambridge, MA 02138, USA

ABSTRACT

The gradual discovery that late Neoproterozoic ice sheets extended to sea level near the equator poses a palaeoenvironmental conundrum. Was the Earth's orbital obliquity > 60° (making the tropics colder than the poles) for 4.0 billion years following the lunar-forming impact, or did climate cool globally for some reason to the point at which runaway ice-albedo feedback created a 'snowball' Earth? The high-obliquity hypothesis does not account for major features of the Neoproterozoic glacial record such as the abrupt onsets and terminations of discrete glacial events, their close association with large (> 10‰) negative $\delta^{13}C$ shifts in seawater proxies, the deposition of strange carbonate layers ('cap carbonates') globally during post-glacial sea-level rise, and the return of large sedimentary iron formations, after a 1.1 billion year hiatus, exclusively during glacial events. A snowball event, on the other hand, should begin and end abruptly, particularly at lower latitudes. It should last for millions of years, because outgassing must amass an intense greenhouse in order to overcome the ice albedo. A largely ice-covered ocean should become anoxic and reduced iron should be widely transported in solution and precipitated as iron formation wherever oxygenic photosynthesis occurred, or upon deglaciation. The intense greenhouse ensures a transient post-glacial regime of enhanced carbonate and silicate weathering, which should drive a flux of alkalinity that could quantitatively account for the world-wide occurrence of cap carbonates. The resulting high rates of carbonate sedimentation, coupled with the kinetic isotope effect of transferring the CO_2 burden to the ocean, should drive down the $\delta^{13}C$ of seawater, as is observed. If cap carbonates are the 'smoke' of a snowball Earth, what was the 'gun'? In proposing the original Neoproterozoic snowball Earth hypothesis, Joe Kirschvink postulated that an unusual preponderance of land masses in the middle and low latitudes, consistent with palaeomagnetic evidence, set the stage for snowball events by raising the planetary albedo. Others had pointed out that silicate weathering would most likely be enhanced if many continents were in the tropics, resulting in lower atmospheric CO_2 and a colder climate. Negative $\delta^{13}C$ shifts of 10–20‰ precede glaciation in many regions, giving rise to speculation that the climate was destabilized by a growing dependency on greenhouse methane, stemming ultimately from the same unusual continental distribution. Given the existing palaeomagnetic, geochemical and geological evidence for late Neoproterozoic climatic shocks without parallel in the Phanerozoic, it seems inevitable that the history of life was impacted, perhaps profoundly so.

Terra Nova, 14, 129–155, 2002

Introduction

In 1987, the Caltech biomagnetist and palaeomagnetist Joe Kirschvink gave undergraduate Dawn Sumner a rock sample to study for her senior thesis. The sample, collected by UCLA palaeontologist Bruce Runnegar, was a reddish, uncompacted, rhythmically laminated siltstone from the Elatina Formation, a late Neoproterozoic, glacial and periglacial unit widely exposed in the Flinders Ranges and elsewhere in South Australia (Preiss, 1987; Lemon and Gostin, 1990). The rhythmic laminations are interpreted to be lunar tidal bundles (Williams, 2000), implying a shallow marine depositional environment. Glacigenic deposits (diamictites and ice-rafted dropstones) occur in most sections of the Elatina Formation (Lemon and Gostin, 1990), but previous palaeomagnetic studies suggested that the siltstone was deposited close to the equator on the basis of unusually stable remnant magnetization carried by detrital haematite (Embleton and Williams, 1986). Kirschvink was skeptical that glaciers would ever reach sea level in the tropics, so he instructed Sumner to perform a fold test (McElhinny and McFadden, 2000) on soft-sediment folds (Williams, 1996) in Runnegar's sample. A positive fold test would prove that the natural remnant magnetization (NRM) is primary; a negative result would show that it is secondary, posing no constraint on the palaeolatitude of the Elatina glaciation. To Kirschvink's surprise, the fold test was positive (Sumner *et al.*, 1987), as others subsequently confirmed (Schmidt *et al.*, 1991; Schmidt and Williams, 1995; Sohl *et al.*, 1999). A stratigraphically consistent, polarity reversal test (Sohl *et al.*, 1999; see also Schmidt and Williams, 1995) confirmed the primary component of NRM in the Elatina Formation, while the existence of multiple reversals (Sohl *et al.*, 1999) suggests that the Elatina glacial epoch lasted for several 10^5 to a few 10^6 years.

The Elatina results refocused attention on Neoproterozoic glaciations. A critical review of the stratigraphic, geochronological and palaeomagnetic constraints on virtually all late Neoproterozoic glacial deposits (LNGD) world-wide was recently published (Evans, 2000). A total of 16 regional-scale units, known to have formed near sea level, possess primary or

*Correspondence: Paul Hoffman, 20 Oxford St., Cambridge, MA 02138, USA. E-mail: hoffman@eps.harvard.edu; fax: +1 617 496 0434.

near-primary NRM components giving at least 'somewhat reliable' palaeolatitudes (Evans, 2000). Many were apparently deposited within 10° of the equator, and none was laid down at a palaeolatitude greater than 60° (Fig. 1). Increased non-dipole components in the Proterozoic geomagnetic field (Kent and Smethurst, 1998; Bloxham, 2000) would not greatly affect those conclusions (Evans, 2000) (Fig. 1). The observations are surprising and they argue that the Elatina result is no fluke.

While LNGD (Fig. 2) closely resemble Phanerozoic glacial deposits lithologically, their distribution and mode of occurrence have never fitted comfortably into Phanerozoic stereotypes (Harland, 1964; Schermerhorn, 1974; Deynoux, 1985; Crowley and North, 1991; Eyles, 1993; Crowell, 1999). LNGD (Fig. 1) are widely distributed on all continents (Mawson, 1949a; Cahen, 1963; Harland, 1964; Hambrey and Harland, 1981; Evans, 2000) and they are sharply interposed in normal marine carbonate successions (Fig. 2c) in several regions (Harland and Wilson, 1956; Schermerhorn and Stanton, 1963; Martin, 1965; Roberts, 1976; Preiss, 1987). Distinctive 'cap' dolostone (and rarely limestone) layers sharply overlie most LNGD without significant hiatus (Fig. 2f), implying a sudden switch back to a warmer climate (Norin, 1937; Mawson, 1949b; Deynoux and Trompette, 1976; Kröner, 1977; Williams, 1979). Cap carbonates (Figs 3–5) have unusual sedimentological, geochemical and isotopic characteristics not found in other Neoproterozoic or Phanerozoic carbonates (Aitken, 1991; Fairchild, 1993; Grotzinger and Knoll, 1995; Kennedy, 1996; James *et al.*, 2001), and they occur even in successions otherwise lacking carbonate (Spencer, 1971; Deynoux, 1980; Plumb, 1981; Myrow and Kaufman, 1999). Not surprisingly, they have long served as time markers in regional and even interregional correlation (Dunn *et al.*, 1971; Kennedy *et al.*, 1998; Walter *et al.*, 2000).

The glacial origin of the Elatina Formation was first recognized by Sir Douglas Mawson – the older, thicker and more localized, Surtian LNGD in the same region were recognized much earlier by Howchin (1908), following the first described LNGD in northern Norway (Reusch, 1891) – and he discovered its cap dolostone (Mawson, 1949b). Although conservative by nature (Sprigg, 1990), Mawson was the first (to our knowledge) to argue that late Neoproterozoic glaciation was global, with large ice sheets in the tropics (Mawson, 1949a). He went on to suggest that climatic amelioration paved the way for the first metazoa (Mawson, 1949a), which had been discovered by a Mawson protegé, Reg Sprigg, in the Ediacara Hills west of the Flinders Ranges (Sprigg, 1947). Ironically (for an Adelaide resident), Mawson was opposed to continental drift, and his argument for tropical ice sheets depended critically on the occurrence of LNGD in tropical Africa today (Mawson, 1949a). [To his credit, Mawson urged students to read his

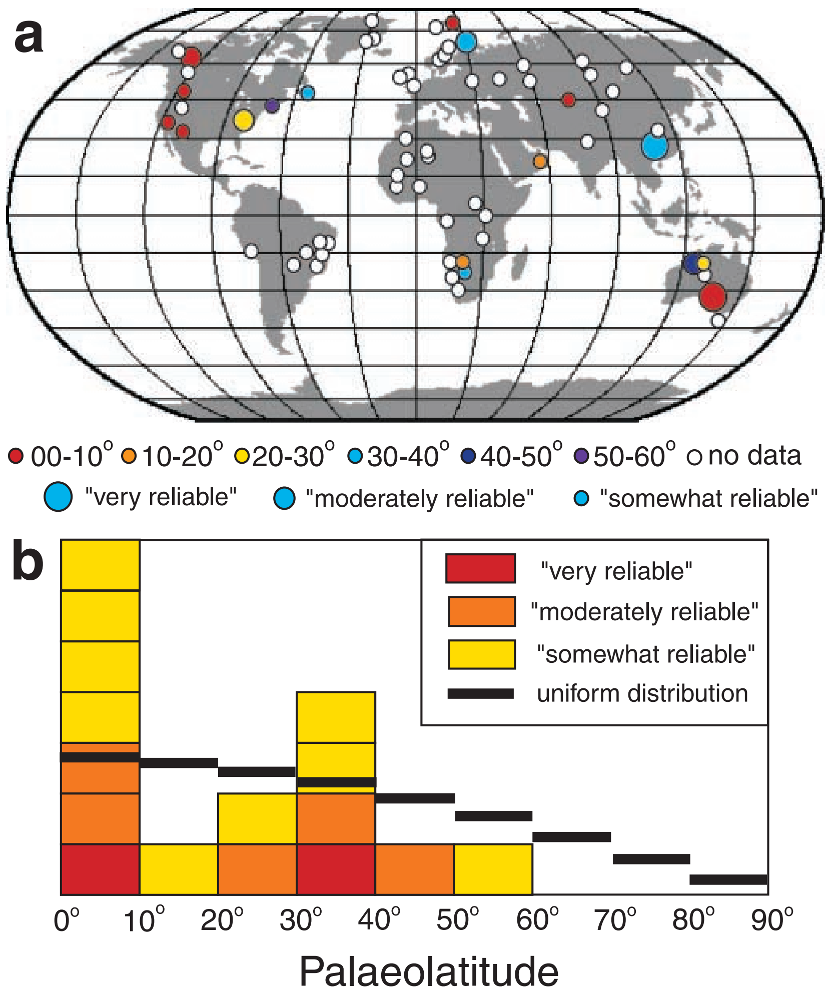

Fig. 1 Global distribution (a) of Neoproterozoic glaciogenic deposits with estimated palaeolatitudes based on palaeomagnetic data (modified from Evans, 2000). 'Reliability' takes into account not only palaeomagnetic reliability but also the confidence that the deposits represent regionally significant, low-elevation ice sheets (Evans, 2000). Histogram (b) of the same glaciogenic deposits according to palaeolatitude. The discontinuous steps show the expected density function of a uniform distribution over the sphere. Note the preponderance of low-latitude deposits and absence of high-latitude deposits. This finding would not be invalidated by plausible non-diplole components of the field, which would effectively raise the palaeolatitudes of only the mid-latitude results (Evans, 2000). The minimum in the distribution in the subtropics may reflect the meridional variation in precipitation minus evaporation due to the Hadley cells.

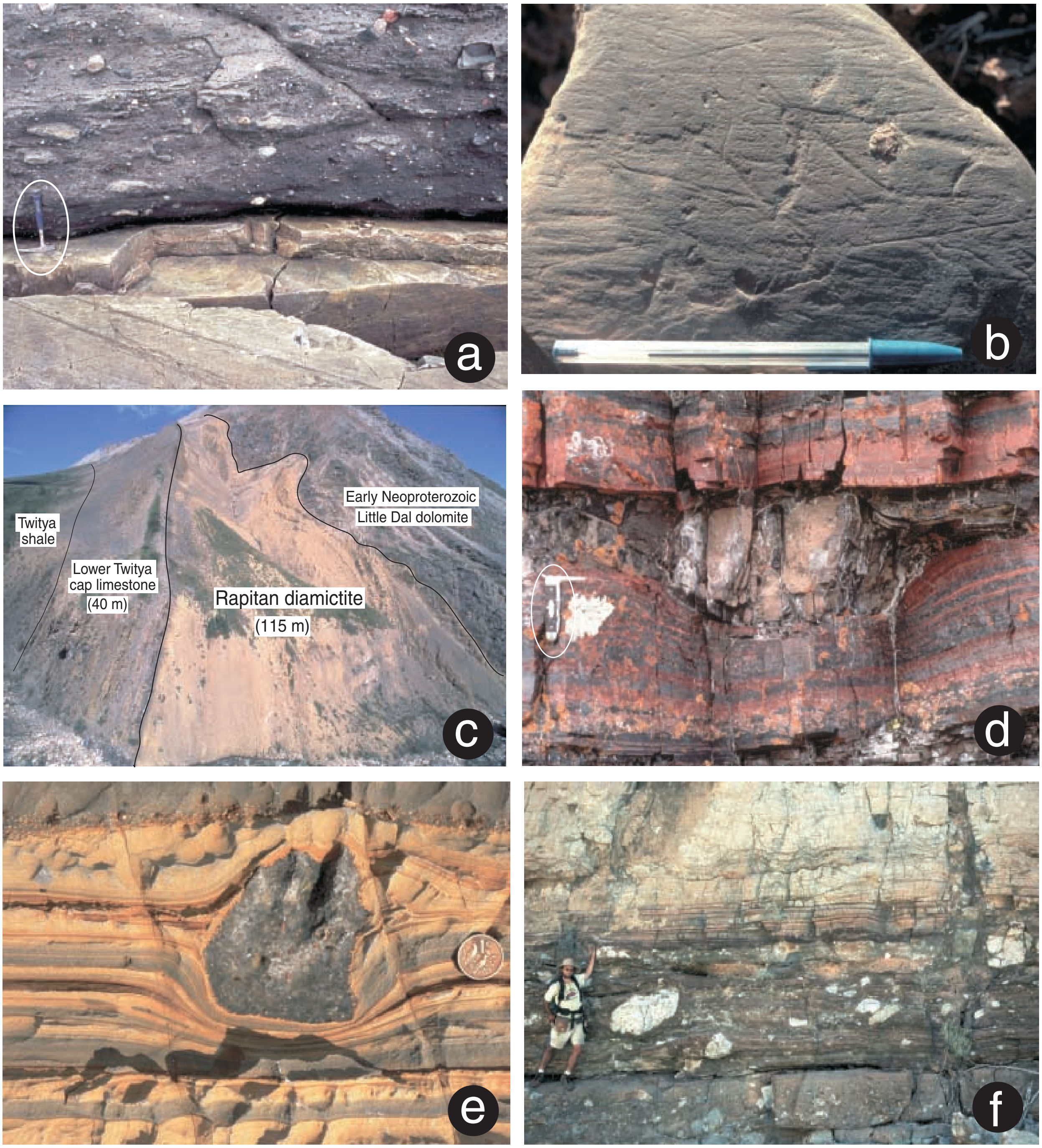

Fig. 2 Neoproterozoic glacial features. Striated pavement (a) overlain by the Smalfjord diamictite (Table 1) at Bigganjargga, Varangerfjord, north Norway, the first recognized Neoproterozoic glacial deposit (Reusch, 1891) (G. P. Halverson photo). Faceted and multistriated stone (b) from the Jbéliat diamictite (Table 1) in Adrar, Mauritania. Rapitan diamictite (Table 1) sharply bounded (c) by carbonate strata, without transitional facies or intercalation at Stone Knife River, Mackenzie Mountains, north-west Canada. Dolomite dropstone in banded iron formation (d) within the Rapitan diamictite at Snake River, Mackenzie Mountains (G. A. Gross photo). Ice-rafted dropstone (e) of shelf-edge oolitic limestone in allodapic slope-facies carbonates of the Ghaub diamictite (Table 1) at east Fransfontein, north-west Namibia. Impact of dropstone on sea-bed caused the folded bicouple seen at 10 o'clock from coin. Typical abrupt conformable contact (f) between the upper dropstone unit of the Ghaub diamictite and its cap dolostone in slope facies at west Fransfontein, north-west Namibia. The coin, pen and hammer are 2, 15 and 33 cm in maximum dimension, respectively (same in Figs 4 and 5).

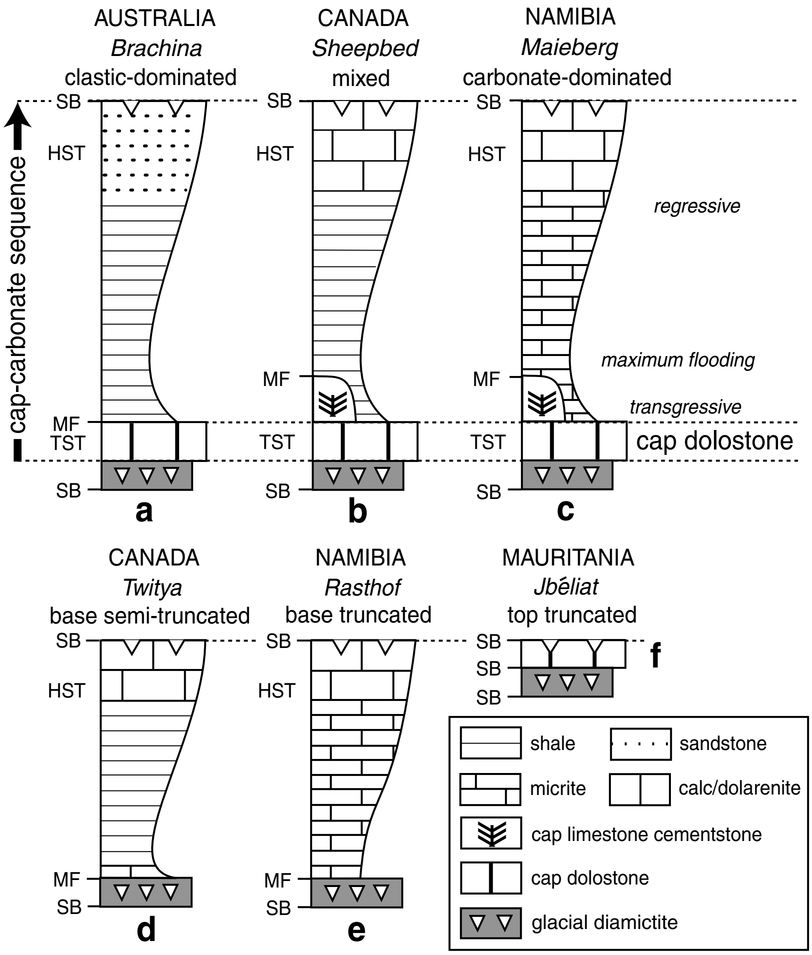

Fig. 3 Schematic variability in cap-carbonate sequences (not drawn to scale). Note distinction between 'cap dolostone' and 'cap-carbonate sequence'. Workers from clastic-dominated (a) regions (e.g. Kennedy, 1996; Kennedy *et al.*, 2001b) regard cap dolostones as the sole representatives of the post-glacial transient. However, unusual textures (e.g. crystal-fan cementstones) occur above the cap dolostone in mixed (b) and carbonate-dominated (c) regions, and the post-glacial negative $\delta^{13}C$ anomaly may encompass the entire cap-carbonate sequence (Fig. 9). The top of the cap dolostone does not mark the end of enhanced silicate weathering (Kennedy *et al.*, 2001b), but may reflect a change from carbonate-dominated to silicate-dominated weathering as carbonate platforms are inundated by rising sea level (Hoffman and Schrag, 2000). Base truncation (d,e) may occur if the local water mass fails to reach saturation until after post-glacial sea-level rise. Top truncation (f) occurs in regions with little background tectonic subsidence to create permanent accommodation space. Abbreviations: HST, highstand systems tract; MF, marine flooding surface; SB, sequence boundary; TST, transgressive sequence tract (van Wagoner *et al.*, 1988).

contemporary's book (Wegener, 1922) and Sprigg, for one, identified the Adelaidean succession as a pre-Mesozoic rifted continental margin (Sprigg, 1952).] Mawson's argument, however, collapsed in the plate tectonic revolution, with most subsequent workers attributing the extent of LNGD (Fig. 1) to rapid drift of different continents through polar regions at different times (Crawford and Daily, 1971; McElhinny *et al.*, 1974; Crowell, 1983, 1999; Eyles, 1993).

Most, but not all. Brian Harland of Cambridge University cut his teeth in the Arctic archipelago of Svalbard, sentinel of the Barents Sea shelf, and host to a pair of LNGD (Harland *et al.*, 1993; Harland, 1997). Harland was no fixist, but he independently reiterated Mawson's arguments (Harland and Rudwick, 1964; Harland, 1964) and reinforced them with palaeomagnetic measurements. Low-inclination NRM in LNGD and associated strata in the North Atlantic region and elsewhere seemed initially to prove that ice sheets had indeed extended to low palaeolatitudes (Harland and Bidgood, 1959; Bidgood and Harland, 1961; Chumakov and Elston, 1989). Later, however, with the recognition of widespread, low-temperature remagnetization (McCabe and Elmore, 1989), field tests and demagnetization procedures that constrain the age and subsequent history of magnetization became the gold-standard for acceptance of palaeomagnetic data (McElhinny and McFadden, 2000). The Elatina Formation was the first LNGD for which there were multiple field, rock-magnetic, and petrographic tests indicative of a primary, low-inclination NRM, contemporaneous with sedimentation (Embleton and Williams, 1986; Sumner *et al.*, 1987; Schmidt *et al.*, 1991; Schmidt and Williams, 1995; Sohl *et al.*, 1999).

Alternative theories for low-latitude glaciation

Kirschvink was not the first to wrestle with the low-latitude Elatina results. George Williams (1975, 1993, 2000) had long advocated a large (> 54°) orbital obliquity, or tilt (the angle between the Earth's axes of rotation and orbit around the sun), to account for low-latitude glaciation in conjunction with inferred strong equatorial seasonality during the Elatina glaciation (Williams and Tonkin, 1985; Williams, 1998). In theory, obliquity could have varied chaotically within 60–90° following the early lunar-forming impact event, but a low obliquity, once achieved, is self-stabilizing through the gravitational interaction of the Moon and the Earth's equatorial bulge (Laskar *et al.*, 1993). Williams (1993) postulates a sharp decrease in orbital obliquity after 600 Ma, with resultant moderation of the seasonal climate cycle giving rise to the metazoa (Williams, 1993). With an obliquity > 54°, mean annual temperatures are lower around the equator than at the poles (Williams, 1975; Hunt, 1982; Oglesby and Ogg, 1999; Jenkins, 2000), making glaciation more probable at lower

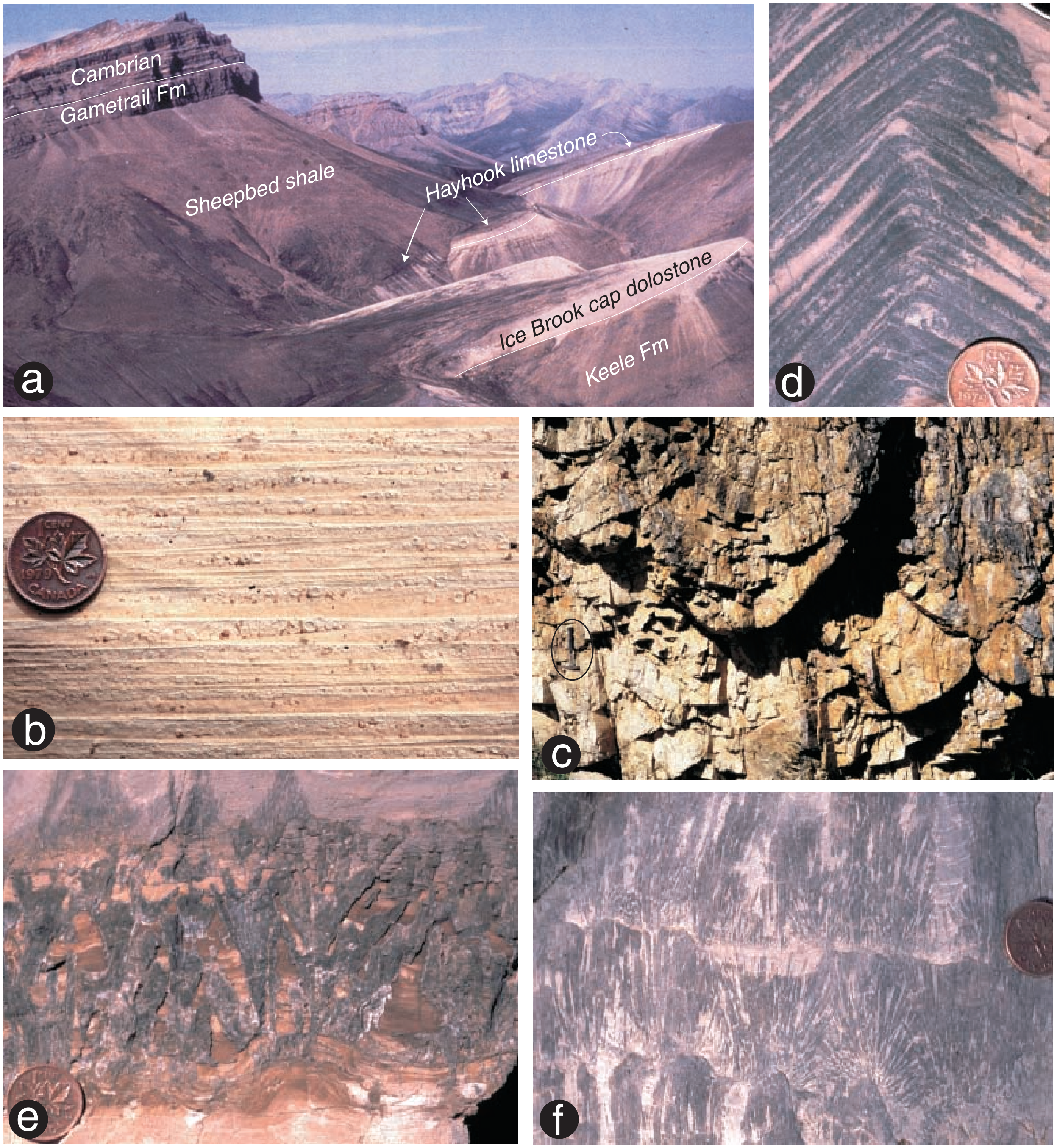

Fig. 4 Distinctive lithofacies in the Ice Brook (Table 1) cap carbonate, Mackenzie Mountains, north-west Canada. The Ice Brook cap-carbonate sequence (a) at Shale Lake includes a very pale, flinty, cap dolostone, locally crowned by dark Hayhook limestone cementstone, then 700–900 m of black, deep-water, Sheepbed shale, shoaling finally to Gametrail dolomite, truncated here by the Lower Cambrian (photo from James *et al*., 2001). Low-angle cross-sets of reverse-graded peloids (b) in the cap dolostone at Gayna River. Cuspate mega-ripples, aka pseudo-tepees (c) in the cap dolostone at Arctic Red River. Axial zone of cuspate mega-ripple (d) at Gayna River, showing evidence of oscillatory (storm wave) currents sweeping across the aggrading crestline. Digitate pseudo-stromatolites composed of sea-floor barite cement (e) at the contact between the cap dolostone and Hayhook limestone at Shale Lake. The slender dark prisms growing off the tips of the barite fingers near the top of the photo are pseudomorphosed aragonite. Crystal fans of aragonite (f), replaced by calcite, and meniscus-laminated micrite in the Hayhook cap limestone at Shale Lake.

latitudes (Williams, 1975). Summer insolation is so large in the polar regions (the sun staying high in the sky throughout the diurnal cycle) that surface temperatures over land areas might exceed the boiling point of water (Oglesby and Ogg, 1999). The tropics, although cooler overall, would have two hot seasons near

Terra Nova, Vol 14, No. 3, 129–155

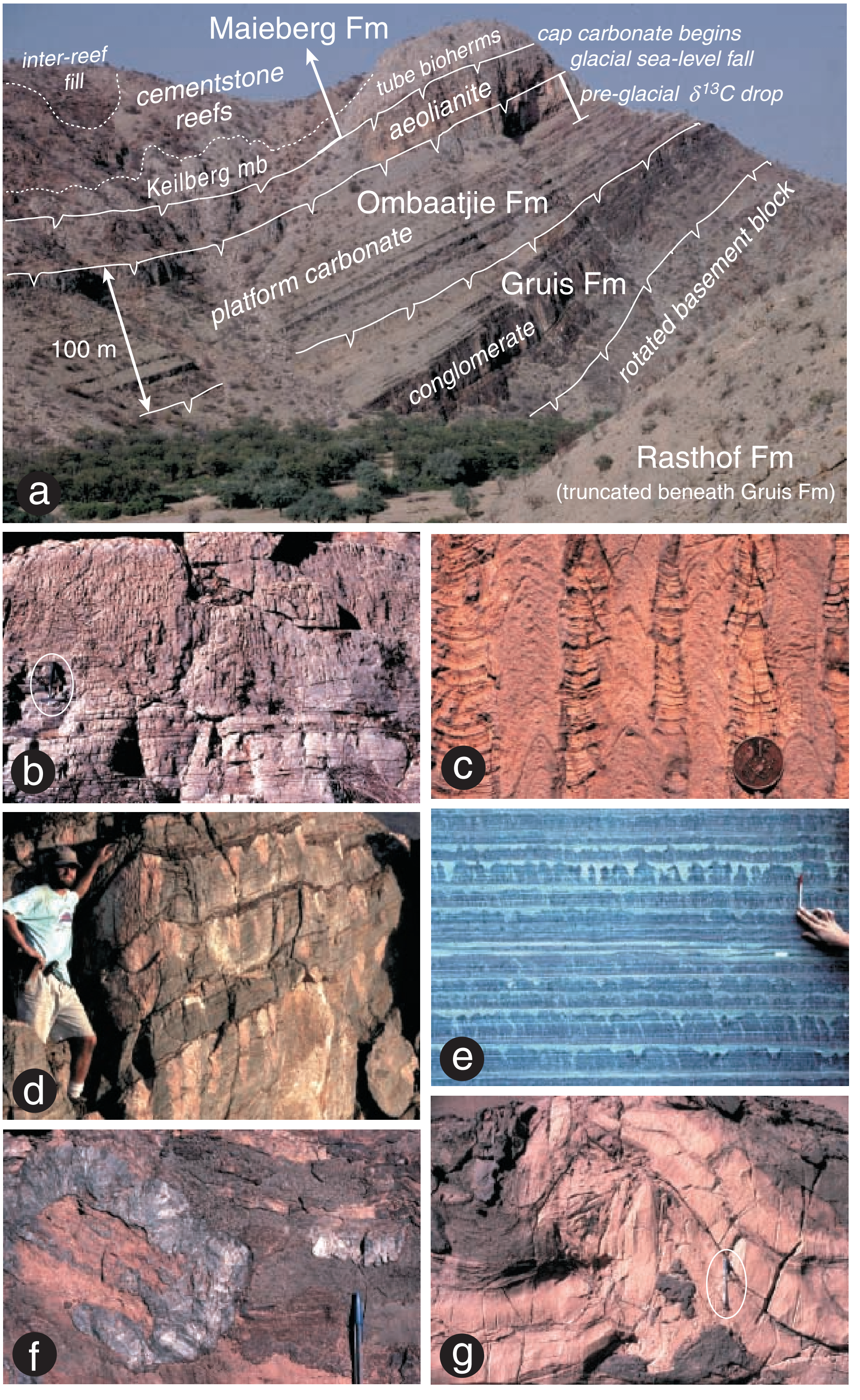

Fig. 5 Distinctive lithofacies in the cap-carbonate sequence (Maieberg Formation) following the Ghaub glaciation (Table 1) of the Otavi platform, northwest Namibia, and possible correlatives. Section (a) near the platform margin at Tweelingskop, showing preglacial drop in $\delta^{13}C$, aeolian dolostone representing the glacial event, mounded cap dolostone (Keilberg member) composed of stromatolites with tube-like structure, and reef-like buildups of sea-floor aragonite cements pseudomorphosed by calcite (Soffer, 1998). Tube-like structures (b) in hummocky cross-stratified cap dolostone at Khowarib Schlucht. Tubes initiated within the cap dolostone and do not tap subglacial deposits as expected if they formed by methane released from glacial permafrost as proposed by Kennedy *et al.* (2001a). Detail of tube-like structures (c) at Khowarib Schlucht showing meniscus-laminated micrite (tubes) filling circular pits within a honeycomb of stromatolites (arched laminae). Despite vertical continuity of tube-like structures (b), synoptic relief during growth was < 3 cm. Sheaves of former-aragonite crystal fans (d) in allodapic limestone at Tweelingskop. Interlayered micrite (light) and aragonite (dark) cements (e) pseudomorphosed to calcite in the Sete Lagoas cap carbonate, Bambuí platform, south-eastern Brazil. Barite crust (f) and reworked barite-crusted clast (above pen) at sequence boundary between Jbéliat (Table 1) cap dolostone and Téniagouri Group (Fig. 10) at Atar Cliffs, Adrar, Mauritania. Unlike sea-floor barite (Fig. 4e), Jbéliat barite appears to be a product of phreatic diagenesis in a supratidal tepee breccia, possibly related to mixing of marine and meteoric groundwaters. True tepee structure (g) formed by layer-parallel expansion due to vadose cementation in supratidal Jbéliat cap dolostone at Atar Cliffs. Jbéliat tepee ridges are polygonal in plan, unlike linear pseudo-tepees (mega-ripples) in sublittoral cap dolostones (Fig. 4c,d).

equinox, when insolation would be indistinguishable from the hottest tropical seasons with low obliquity (Oglesby and Ogg, 1999). Indeed, hot summers and strong seasonality make glaciation problematic at any latitude with large obliquities (Hoffman and Maloof, 1999). It does, however, provide a ready but non-unique (Maloof *et al.*, 2002) explanation for the existence of well-developed, periglacial, sand-wedge polygons in the Elatina Formation (Williams and Tonkin, 1985). These structures are most easily explained as resulting from large seasonal oscillations in soil temperature (Lachenbruch, 1962), which should not occur near the equator if the obliquity was close to its present value of 23.5°. On the other hand, a persistent large obliquity does not explain the characteristically abrupt onsets and terminations of LNGD (Hambrey and Harland, 1981; Preiss, 1987; Narbonne and Aitken, 1995; Hoffmann and Prave, 1996; Hoffman *et al.*, 1998a). Nor does it account for the close association of LNGD with carbonates, because the 'redistribution of the radiant energy balance to polar latitudes should also move the carbonate belts from equatorial latitudes to the poles, where the glaciers (in Williams' model) should not encounter them' (Kirschvink, 1992). The dynamics of the postulated obliquity reduction after 600 Ma remain conjectural (Williams, 1993; Ito *et al.*, 1995; Néron de Surgy and Laskar, 1997; Williams *et al.*, 1998; Pais *et al.*, 1999).

Richard Sheldon (1984) postulated that orbiting ice rings episodically collapsed into the atmosphere, transiently shielding sunlight and giving rise to glaciers at low latitudes. The theory strives to explain iron formations and cap carbonates, but does not adequately account for low-latitude glaciation. Due to orbital obliquity, equatorial ice rings will cast shadows only on the winter hemisphere (see figure 2 in Sheldon, 1984). Glaciation depends critically on cool summers, not cold winters (Köppen and Wegener, 1924), as it is contingent on a fraction of the annual snowfall surviving the melting seasons.

Snowball Earth

Kirschvink responded to the positive Elatina fold test with a theory he first aired in 1989 (Maugh, 1989). It eventually appeared as an article, seven paragraphs long, embedded in a 1348-page book (Kirschvink, 1992). It postulated that conditions amenable to global glaciation were set up by an unusual preponderance of land masses within middle to low latitudes, a situation that has not been encountered at any subsequent time in Earth history. One effect of such a palaeogeography would be a substantially higher albedo in the subtropics, where clouds are least important (Kirschvink, 1992). Any resultant glaciation would further increase the Earth's albedo by lowering sea level, exposing continental shelves and inland seas (Kirschvink, 1992). Placing more continents in the tropics would also increase the silicate weathering rate (provided tectonic uplift was not mysteriously absent there), leading to a colder planet with lower atmospheric pCO_2 (Marshall *et al.*, 1988; Worsley and Kidder, 1991). In addition, the meridional heat transport by the Hadley cells would be weakened because tropical air masses would be drier on average with greater continentality. Oceanic heat transport might also be lessened, but this is less certain. These combined effects might lead to the growth of large ice caps, nucleated on islands or continents bordering the polar seas.

Ice caps create a positive feedback on climate change through ice-albedo feedback (Croll, 1867; Budyko, 1966; Manabe and Broccoli, 1985). Early energy-balance climate models revealed a fundamental instability in the climate system caused by this positive feedback (Eriksson, 1968; Budyko, 1969; Sellers, 1969; North *et al.*, 1981), an effect reproduced in a number of GCMs (Wetherald and Manabe, 1975; Jenkins and Smith, 1999; Hyde *et al.*, 2000; Pollard and Kasting, 2001). If more than about half the Earth's surface area were to become ice covered, the albedo feedback would be unstoppable (Fig. 6). Surface temperatures would plummet (Fig. 7), and pack ice would quickly envelope the tropical oceans (Hyde *et al.*, 2000; Baum and Crowley, 2001). With reduced Neoproterozoic solar forcing, the ice-albedo instability occurs in the GENESIS v2 GCM between 1.0 and 2.5 times modern pCO_2 with different palaeogeographies (Baum and Crowley, 2001; Pollard and Kasting, 2001). The time scale of the sea-ice advance is uncertain – the ocean's thermal inertia resists the ice advance initially (Poulsen *et al.*, 2001), but the ocean is a finite heat reservoir and cooling over thousands

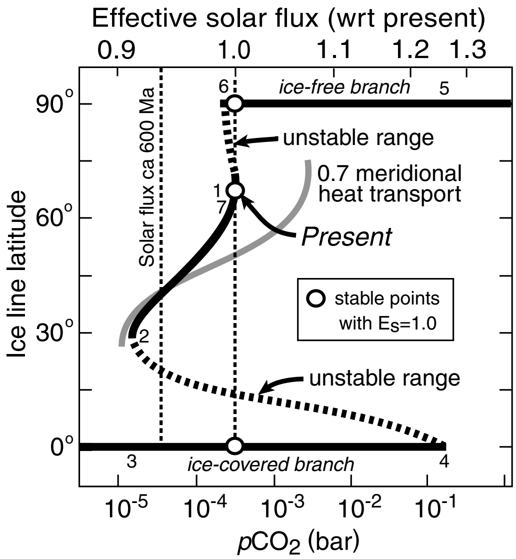

Fig. 6 Ice-line latitudes (at sea level) as a function of the effective solar flux (E_s), or equivalent pCO_2 (for $E_s = 1.0$), based on a simple energy-balance model of the Budyko-Sellers type (after Caldeira and Kasting, 1992; Ikeda and Tajika, 1999). Effect of a 30% reduction in meridional heat transport is shown, as is the estimated solar flux at ~ 600 Ma. Of three possible stable points for $E_s = 1.0$, the Earth actually lies on the partially ice-covered branch at point 1. An instability due to ice-albedo feedback drives any ice-line latitude < 30° onto the ice-covered branch. A $pCO_2 \approx 0.12$ bar is required for deglaciation of an ice-covered Earth, assuming the planetary albedo is 0.6 and $E_s = 1.0$ (Caldeira and Kasting, 1992). The snowball Earth hypothesis is qualitatively predicated on these findings and infers a hysteresis in pCO_2 (and consequently surface temperature) following the circuit labelled 1–7. Starting from point 1, lowering of pCO_2 causes ice lines to migrate stably to point 2, whereupon runaway ice-albedo feedback drives ice lines to the ice-covered branch at point 3. Normal volcanic outgassing over millions of years increases pCO_2 to point 4, initiating deglaciation. Reverse ice-albedo feedback then drives ice lines rapidly to the ice-free branch at point 5, where high pCO_2 combined with low planetary albedo creates a transient ultra-greenhouse. Enhanced silicate weathering causes lowering of pCO_2 to point 6, whereupon polar ice caps reform and ice lines return to the partially ice-covered branch at point 7. In the 1960s, Budyko was concerned with the small ice-cap instability, which predicts a possible switch to the ice-free branch (e.g. disappearance of Arctic sea ice) due to anthropogenic global warming.

of years would leave it powerless to resist the ice encroachment. It is also uncertain if the tropical ocean would ever become entirely ice covered (Hyde *et al.*, 2000; Baum and Crowley, 2001; Warren *et al.*, 2002) Kirschvink (1992) speculated that areas of open water (polynyas) would remain, tracking the zone of highest solar incidence back and forth across the equator and imparting a strongly seasonal climate even at low latitude, consistent with geological observations (Williams and Tonkin, 1985). This is distinct from the tropical 'loophole' model (Hyde *et al.*, 2000; Baum and Crowley, 2001; Crowley *et al.*, 2001), in which the ice fronts miraculously approach but never cross the ice-albedo instability threshold [but the continents are glaciated because they are mostly placed in middle and high latitudes, contrary to palaeomagnetic evidence (Evans, 2000)].

Assuming an albedo runaway did occur, the climate would be dominated by the dry atmosphere and the low heat capacity of the solid surface (Walker, 2001). It would be more like Mars (Leovy, 2001) than Earth as we know it, except that the greater atmospheric pressure would allow surface meltwater to exist. Diurnal and seasonal temperature oscillations would be strongly amplified at all latitudes because of weak lateral heat transfer and extreme 'continentality' (Walker, 2001). Despite mean annual temperatures well below freezing everywhere, afternoon temperatures in the summer hemisphere would reach the melting point (Walker, 2001). Evaporation of transient melt water would contribute, along with sublimation, to maintain low levels of atmospheric water vapour, and glaciers would feed on daily updrafts of this moisture (Walker, 2001). The global mean thickness of sea ice depends strongly on sea-ice albedo (~ 1.4 km for albedo 0.6) and meridional variability is a complex function of solar incidence, greenhouse forcing (see below), zonal albedo, ablation or precipitation, and equatorward flowage of warm basal ice (Warren *et al.*, 2002).

Climate physicists originally assumed that no ice-albedo catastrophe ever actually occurred because it would be permanent: the high planetary albedo would be irreversible. A saviour exists, however, and Kirschvink (1992) identified it as the buildup of an intense atmospheric CO_2 greenhouse through the action of plate tectonics in driving the long-term carbon cycle (Walker *et al.*, 1981; Caldeira and Kasting, 1992; Kirschvink, 1992). On a snowball Earth, volcanoes would continue to pump CO_2 into the atmosphere (and ocean), but the sinks for CO_2 – silicate weathering and photosynthesis – would be largely eliminated (Kirschvink, 1992). Even if CO_2 ice precipitated at the poles in winter, it would likely sublimate away again in summer (Walker, 2001). CO_2 levels would inexorably rise and surface temperatures would follow, most rapidly at first and more slowly later on (Fig. 7) due to the non-linear relation between CO_2 concentration and the resultant greenhouse forcing (Caldeira and Kasting, 1992). With rising surface temperatures, sea ice thins but ground ice sheets expand in some areas due to a stronger hydrological cycle. If CO_2 outgassing rates were broadly similar to today (a reasonable assumption for 600–700 Ma), then the time needed to build up the estimated 0.12 bar CO_2 required to begin permanent melting at the equator, assuming a planetary albedo of 0.6, would be a few million years (Caldeira and Kasting, 1992; Crowley *et al.*, 2001). This estimate (Fig. 7), while subject to large uncer-

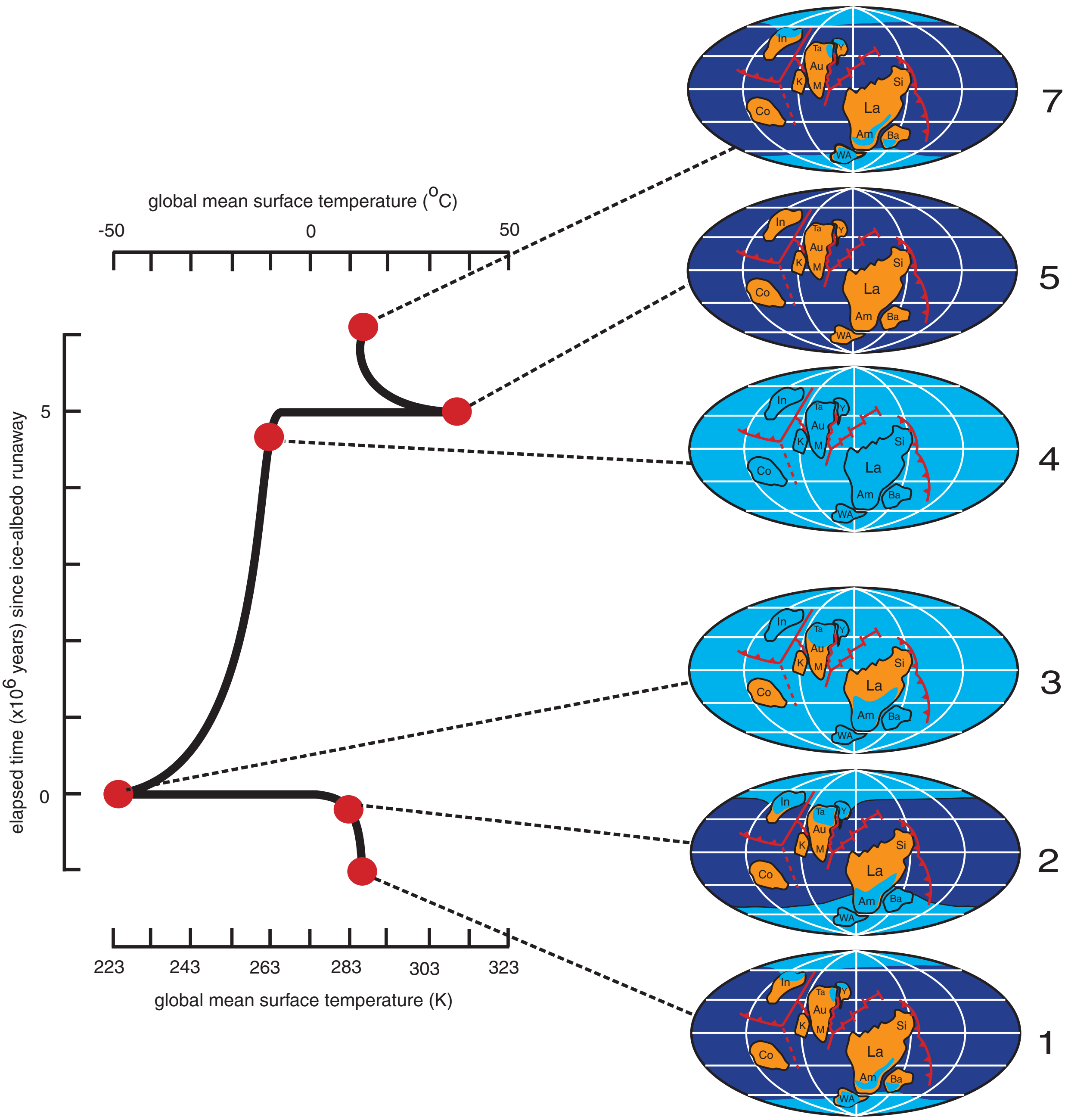

Fig. 7 Estimated changes in global mean surface temperature, based on energy-balance calculations, and ice extent through one complete snowball event. The suggested time scale of the event of ~ 5 Myr is conservative for an albedo = 0.6, based on the estimated outgassing flux of CO_2 and subsidence analysis (Hoffman *et al.*, 1998b). The global palaeogeographical model (Powell *et al.*, 2001) pertains to 750 Ma, ~ 30 Myr before the 'Sturtian' glaciation (Table 1). Palaeocontinents: Am, Amazonia; Au, Australia; Ba, Baltica; Co, Congo; In, India; K, Kalahari; M, Mawson; Si, Siberia; Ta, Tarim; WA, West Africa; Y, South China (Yangtse). The global ice-line depictions correspond approximately to points 1–7 in Fig. 2. Note the growth of terrestrial ice sheets with rising surface temperature during the snowball event. Note also the abrupt onset and termination of glacial conditions in the low and middle latitudes, consistent with geological observations, and the saw-tooth form of the temperature curve reversed to that associated with late Quaternary glacial cycles. Note finally that the estimated surface temperatures are global mean values and give no sense of the real zonal, seasonal and diurnal ranges in temperature (Walker, 2001).

tainties, is of the same order as the estimated time-scale of LNGD from palaeomagnetic (Sohl *et al.*, 1999) and stratigraphic (Hoffman *et al.*, 1998a) evidence. Once the tropical ocean begins to open up perennially, deglaciation proceeds rapidly due to reverse ice-albedo feedback (Caldeira and Kasting, 1992; Crowley *et al.*, 2001).

The fall in planetary albedo occurs far faster than the excess atmospheric CO_2 can be consumed by silicate weathering, with the result that a transient heat wave must follow the ice retreat (Caldeira and Kasting, 1992; Kirschvink, 1992). Kirschvink (1992) concluded that a cold planet with many tropical continents and large polar sea-ice caps 'would be a rather unstable situation, with the potential for fluctuating rapidly between the "ice house" and "greenhouse" states'.

Testing the snowball hypothesis

Kirschvink (1992) highlighted three implications of his theory which 'might lend themselves to geological tests'. First, 'glacial units should be more or less synchronous Harland, 1964)'. Second, 'strata from widely separate areas which preserve a record of these [rapid] climatic fluctuations [between "ice house" and "greenhouse" states] might bear an overall similarity in lithologic character, which would be a result of the global scale of the climatic fluctuations'. Third, 'the presence of floating pack ice should reduce evaporation, act to decouple oceanic currents from wind patterns and, by inhibiting oceanic to atmospheric exchange of O_2, would enable the oceanic bottom waters to stagnate and become anoxic. Over time, ferrous iron generated at the mid-oceanic ridges or leached from the bottom sediments would build up in solution and, when circulation became reestablished toward the end of the glacial period, the iron would oxidize to form a "last-gasp" blanket of banded iron formation in upwelling areas.' Here is how these tests turned out.

Test 1: carbon isotopes

Direct radiometric testing of predicted glacial synchroneity has not proved possible (Table 1) because of an apparent dearth of suitable material for dating (Evans, 2000). Low diversity and turnover rates of microfloral and protistan remains pose severe limits on biostratigraphic resolution until after the major Neoproterozoic glacial events (Knoll, 2000). Regardless, a sea change in favour of synchronous glaciation occurred in the 1990s, and carbon isotope stratigraphy was principally responsible.

The history of carbon isotopic variation (expressed as $\delta^{13}C$, the difference in per mil of $^{13}C/^{12}C$ with respect to standard VPDB) in marine carbonates and covarying organic matter is a robust, but ambiguous, record of biogeochemical cycling (Summons & Hayes, 1992). Despite the fact that significant spatial heterogeneity in $\delta^{13}C$ is dynamically maintained within the ocean (Kroopnick, 1985), large secular changes in $\delta^{13}C$ at individual sites are globally correlated (Veizer *et al.*, 1999; Saltzman *et al.*, 2000), reflecting the residence time of carbon $\sim$ 150 times the ocean mixing time (Kump and Arthur, 1999). The $\delta^{13}C$ of carbonate rocks is relatively immune from large diagenetic changes because pore fluids are effectively buffered by the large rock carbon reservoir (Veizer *et al.*, 1999).

The range of secular $\delta^{13}C$ variability of $> 10‰$ in the late Neoproterozoic (Jacobsen and Kaufman, 1999; Walter *et al.*, 2000) is markedly greater than for the Phanerozoic (Veizer *et al.*, 1999) or the 1.5 billion years before the late Neoproterozoic (Brasier and Lindsay, 1998; Kah *et al.*, 2001). The largest Neoproterozoic $\delta^{13}C$ anomalies consistently bracket LNGD (Figs 8 and 9), with enriched values ($\delta^{13}C_{carb} > 5‰$) observed prior to glaciation and depleted values ($\delta^{13}C_{carb} < 0‰$) afterwards. A steep decline in $\delta^{13}C$ values of 10–15‰ precedes any physical evidence of glaciation or sea-level fall in many areas (Narbonne and Aitken, 1995; Hoffman *et al.*, 1998b; Brasier and Shields, 2000; McKirdy *et al.*, 2001; Xiao *et al.*, 2001; Halverson *et al.*, 2002). Cap carbonates are universally depleted, in some cases approaching mantle values of $-6 \pm 1‰$ (Knoll and Walter, 1992; Kaufman and Knoll, 1995; Kennedy, 1996; Kaufman *et al.*, 1997; Hoffman *et al.*, 1998b; Prave, 1999a; Brasier and Shields, 2000; Walter *et al.*, 2000; James *et al.*, 2001). Although interpretations of these remarkable *trans*-glacial isotopic shifts differ widely (see below), there is consensus that they are supra-regional in nature. Even those opposed to the snowball hypothesis (Kennedy *et al.*, 1998, 2001a,b; Prave, 1999a,b; Condon and Prave, 2000) agree on the synchroneity of glacial events in widely separate areas (Africa, Australia, Canada, Europe) and base global correlation schemes upon them.

The conventional explanation for Neoproterozoic carbon isotopic oscillations and cap carbonates is oceanographic (Knoll *et al.*, 1986, 1996; Kaufman *et al.*, 1991, 1997; Derry *et al.*, 1992; Grotzinger and Knoll, 1995; Grotzinger and James, 2000). The idea is roughly the following. The ocean was physically stratified for long periods pending glaciation, but switched to a turnover mode during and particularly after glacial events. In stratified mode, the biological pump (descent of organic particles from the surface) drove the $\delta^{13}C$ of dissolved inorganic carbon (DIC) in the surface waters to higher values. Partial remineralization of the organic 'rain' in conjunction with bacterial sulphate reduction in the water column produced deep water laden with ^{13}C-depleted DIC. With prolonged stratification, the contrast in $\delta^{13}C$ values between the surface and deep water DIC reservoirs (2–3‰ in the present ocean, Kroopnick, 1985) increased to $> 10‰$, consistent with the preglacial high $\delta^{13}C$ values (Fig. 8). When turnover began, anoxic, alkalinity-laden, deep water upwelled to the surface, releasing CO_2 and precipitating cap carbonates with low $\delta^{13}C$ values. Like the snowball hypothesis, the ocean 'turnover' model (Grotzinger and Knoll, 1995; Knoll *et al.*, 1996) seeks to explain many of the salient observations, but the basic premise is faulty. First, it is physically difficult if not impossible to shut down the overturning circulation for periods > 1.5 kyr (Zhang *et al.*, 2001). Second, organic productivity would crash if the nutrient-rich upwelling flux were removed (Hotinski *et al.*, 2001). Consequently, stratification would not raise the $\delta^{13}C$ in surface waters to 5–10‰, as is observed. Third, cap carbonates formed during post-glacial sea-level rise (see below), when the injection of glacial meltwater would suppressed not enhance, ocean turnover. Kennedy (1996) attributes cap carbonates and their low $\delta^{13}C$ values simply to post-glacial sea-level rise, but his model also depends on an 8–10‰ difference in $\delta^{13}C$ across the thermocline, compared with $\sim$ 2.5‰ for Mesozoic–Cenozoic oceans.

Table 1 Radiometric age constraints on Neoproterozoic glacial events

Region (succession)	Palaeocontinent	Age (Ma)	Glaciation	Age (Ma)	Glaciation	Age (Ma)	Glaciation	Age (Ma)	Glaciation?	Age (Ma)
			'Varanger'		'Marinoan'		'Sturtian'			
1. N Norway (Verstertana)	Baltica	*560**	Mortensnes		Smalfjord	*630**				
2. NE Svalbard (Hecla Hoek)	Laurentia		Wilsonbreen		Elbobreen					
3. SW Scotland (Dalradian)	Laurentia		Loch na Cille	601 ± 4	Port Askaig					
4. US Appalachians (Blue Ridge)	Laurentia	570				700–730	Konnarock	742 ± 2		
5. New England, USA (Boston)	Avalaon	570	Squantum	595 ± 2						
6. Newfoundland (Conception)	Avalon	565 ± 3	Gaskiers	604 + 4/-3						
7. Mauritania (Jbéliat)	West Africa			*595**	**Jbéliat**	*630**				
8. Oman (Huqf)	Arabia				Shuram		Gubrah	723 + 16/-10		
9. NW China (Quruqtagh)	Tarim				Hankalchoug		Tereeken			
10. South China (Sinian)	South China				Nantuo		Jiankou	748 ± 12		
11. South Australia (Adelaide)	Aus-Maws				**Elatina**		**Sturtian**			777 ± 7
12. NW Australia (Kimberley)	Aus-Maws		Egan		Landrigan		Walsh			
13. SW Namibia (Gariep)	Kalahari				Numees			741 ± 6	Kaigas	772 ± 5
14. NW Namibia (Otavi)	Congo				**Ghaub**		**Chuos**	746 ± 2		
15. SW USA (Death Valley)	Laurentia		Rainstorm		Wildrose		Surprise			
16. NW Canada (Windermere)	Laurentia				**Ice Brook**		**Rapitan**	755 ± 18		778 ± 2

All ages U–Pb zircon, except Rb–Sr fine-mica ages (*). For primary sources see: 1. Gorokhov *et al.* (2001); 2. Harland (1997); 3. Dempster *et al.* (2002); 4. Evans (2000); 5. Thompson and Bowring (2000); 6. Myrow and Kaufman (1999); 7. Clauer (1987); 8. Brasier *et al.* (2000); 9. Norin (1937); 10. Evans (2000); 11. Walter *et al.* (2000); 12. Grey and Corkeron (1998), Li (2000); 13. Frimmel *et al.* (2002) [McMillan (1968) would place Kaigas post-741±6 Ma]; 14. Hoffman *et al.* (1996); 15. Corsetti and Kaufman (in press); 16. Narbonne and Aitken (1995). Correlation of glaciations by column is rather arbitrary due to meagre radiometric age constraints. Glacials in bold type are discussed in the text.

In 1998, we invoked the snowball hypothesis, then in eclipse, as a possible explanation for the $\delta^{13}C$ profiles (Figs 8 and 9) of carbonates bounding glacial horizons in northern Namibia (Table 1). Hoffman *et al.* (1998b) gave three, mutually compatible explanations for the ^{12}C enrichment observed in cap carbonates. First, organic productivity on snowball Earth would be greatly reduced for 10^6–10^7 years, which should cause $\delta^{13}C$ values to shift towards the hydrothermal CO_2 input (-6 ± 1‰ VPDB, Des Marais and Moore, 1984) at mid-ocean ridges (Kump, 1991). Second, if carbonate sedimentation rates globally were very high, due to the alkalinity flux from weathering in the greenhouse transient, the organic fraction of the burial flux would be negatively effected. Consequently, carbonate would have low $\delta^{13}C$ values even if organic productivity had fully recovered from the snowball event (Hoffman and Schrag, 1999). Third, the transfer of atmospheric CO_2 to bicarbonate (via the weathering cycle) involves an $\sim$ 8‰ isotopic fractionation favouring ^{13}C. In transferring $>$ 98% of the built-up atmospheric CO_2 to the ocean and ultimately the sedimentary reservoir, the kinetic isotope effect (Rayleigh distillation) will drive the atmospheric CO_2 reservoir to ever lower $\delta^{13}C$ values (Hoffman *et al.*, 1998b). To the degree that atmospheric CO_2 remains a major source of DIC, this would be reflected by cap-carbonate $\delta^{13}C$ values that decline with time (Fig. 8). However, the nadir in $\delta^{13}C$ (Fig. 9) does necessarily correspond to the completion of atmospheric CO_2 drawdown, as Kennedy *et al.* (2001b) argue, but reflects the net effect of many factors, including those already mentioned, as well as methane hydrate destabilization during deglaciation (Kaufman *et al.*, 1997; Kennedy *et al.*, 2001a; but see Hoffman *et al.*, 2002a) and dolomite–calcite isotopic equilibrium.

The swing to negative $\delta^{13}C$ values observed beneath the glacial deposits in many regions (Figs 8 and 9) must originate differently (Kennedy *et al.*, 2001b; Halverson *et al.*, 2002; Schrag *et al.*, 2002) as they are separated in time from the cap-carbonate anomalies by the glacial periods which were of long duration (Hoffman *et al.*,

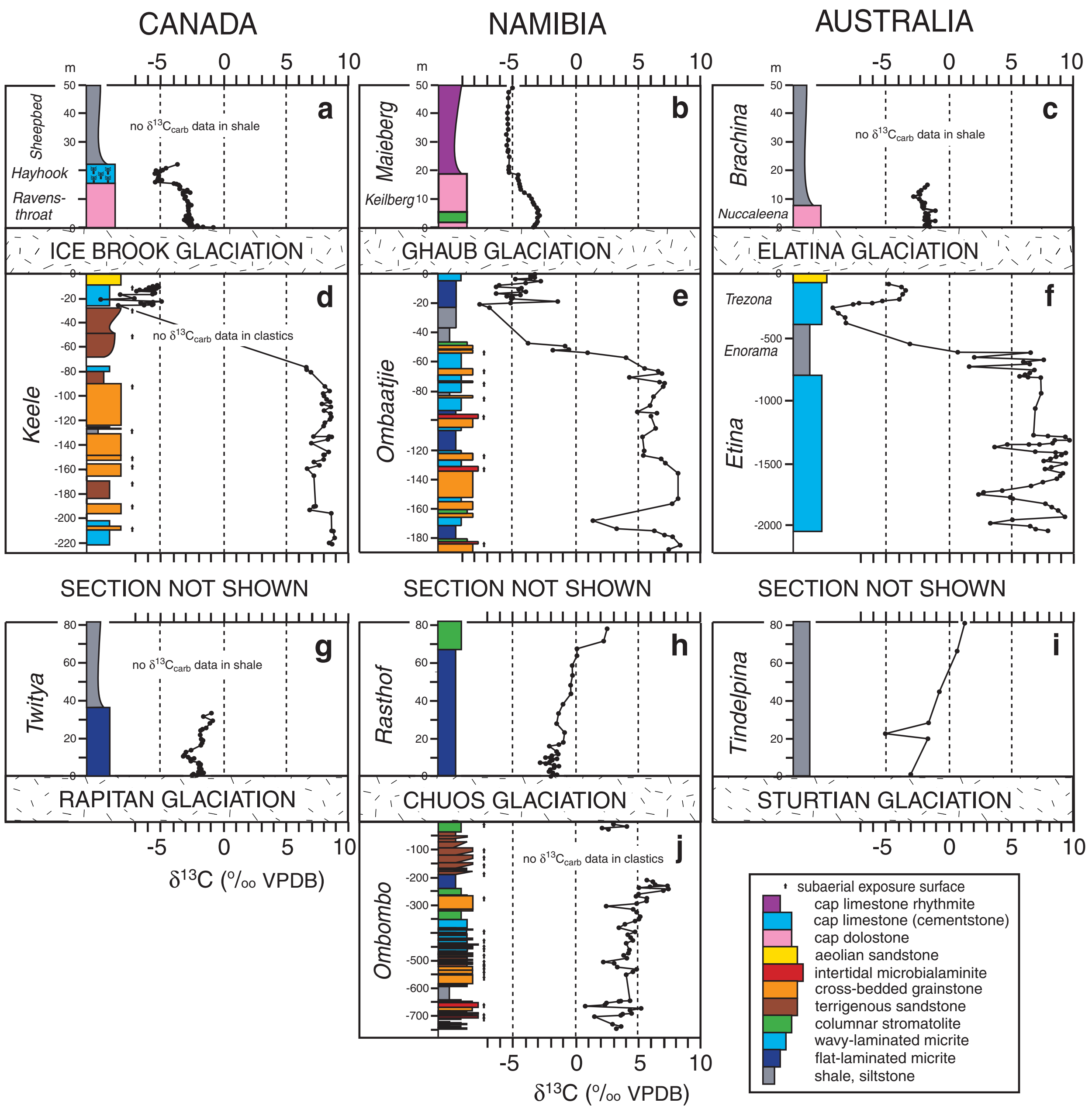

Fig. 8 Representative $\delta^{13}C$ profiles for carbonates bounding the older and younger Neoproterozoic glacials (Table 1) in the northern Canadian Cordillera (left), the Otavi platform in Namibia (centre), and the Adelaide succession in South Australia (right). Note high values (> 5‰) before glaciation and low values (< 0‰) afterwards, and the drop in values that leads the younger glaciation. Correlation follows Kennedy *et al.* (1998). Sources of data are (a) James *et al.* (2001) Redstone section, (b) unpublished Khowarib Schlucht section, (c) unpublished Parachilna Gorge section, (d) unpublished Stone Knife River section, (e) Hoffman *et al.* (1998b) and unpublished Keiserfontein section, (f) McKirdy *et al.* (2001), (g) unpublished Stone Knife River section, (h) unpublished Ombonde River section, (i) McKirdy *et al.* (2001), (j) unpublished Omutirapo section. Note non-uniform thickness scales in panels d–f.

1998a; Sohl *et al.*, 1999). We will discuss the preglacial anomalies, both positive and negative (Fig. 8), and the larger problem of how snowball events originate, in the penultimate section of the paper.

Test 2: cap carbonates

Most LNGD are capped by continuous layers (Figs 3–5) of pure dolostone (and locally limestone), metres to tens of metres thick (Spencer and Spencer, 1972; Williams, 1979; Deynoux, 1980; Fairchild and Hambrey, 1984; Miller, 1985; Preiss, 1987; Aitken, 1991; Fairchild, 1993; Brookfield, 1994; Grotzinger and Knoll, 1995; Kennedy, 1996; Hoffman *et al.*,

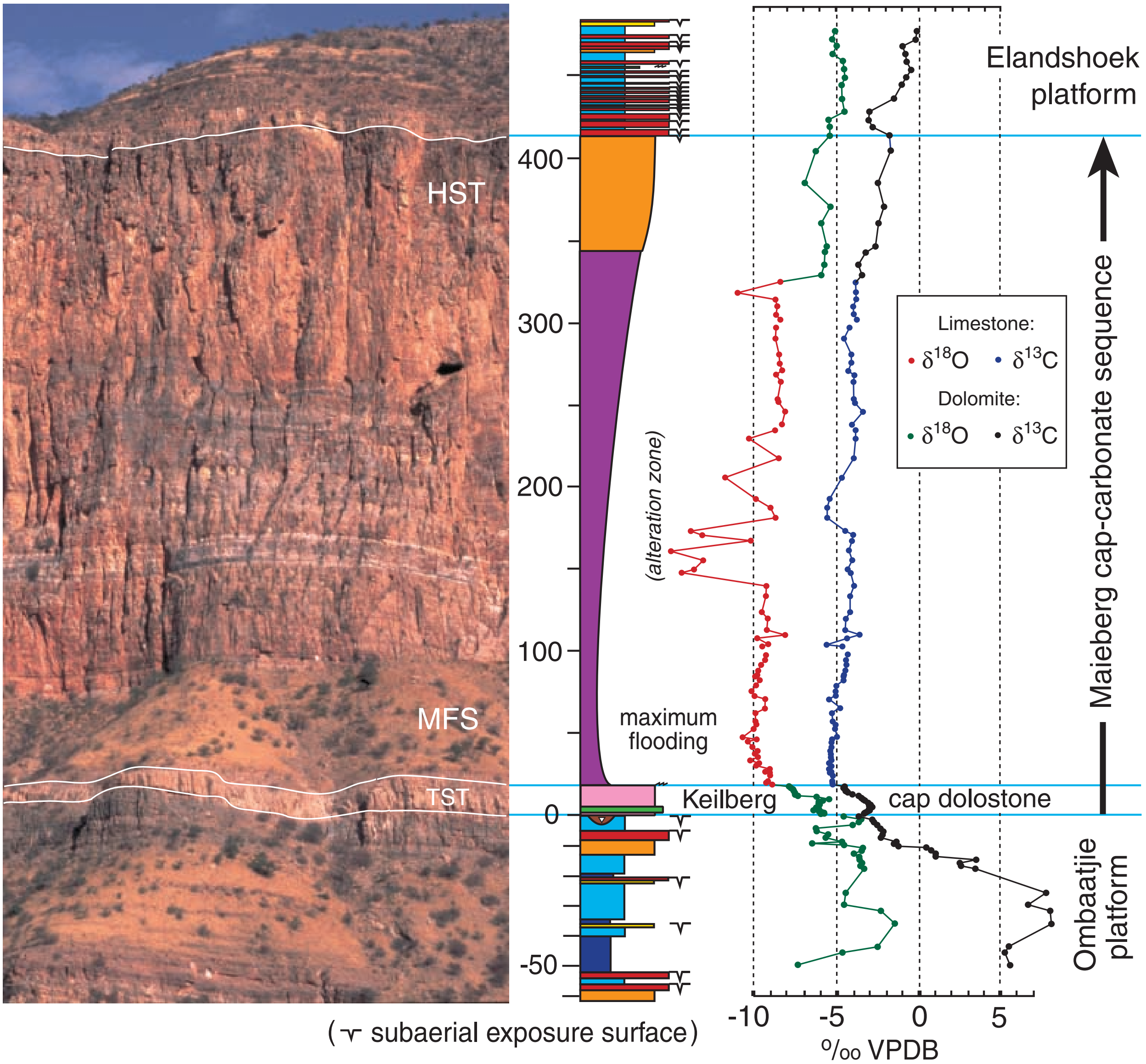

Fig. 9 New representative $\delta^{18}O$ and $\delta^{13}C$ profiles for carbonates bounding the Ghaub (Table 1) glacial surface on the Otavi platform (Khowarib Schlucht section) in northern Namibia. Pockets of diamictite occur sparingly on the glacial surface overlain by the Keilberg cap dolostone. High $\delta^{13}C$ values > 5‰ prevail for ~ 460 m beneath the preglacial drop, which is erosionally truncated in this section compared with that shown in Fig. 8(e). Section was measured and collected on the back side of the ridge shown, where the recessive interval of maximum flooding is continuously exposed. Change in scale at the datum is necessitated by the photographic perspective. Lithofacies as in Fig. 8.

1998a; Corkeron and George, 2001; James *et al.*, 2001). Their basal contacts are characteristically abrupt (Figs 2c, 2f, 4a and 5a), with little evidence of reworking or significant hiatus (Norin, 1937; Williams, 1979; Eisbacher, 1981; Deynoux, 1982; Preiss, 1987; Hoffman *et al.*, 1998a; Brasier *et al.*, 2000). Cap dolostones are transgressive and they typically extend far beyond the confines of their antecedent glacial deposits, blanketing preglacial rocks disconformably (Wright *et al.*, 1978; Preiss, 1987; Aitken, 1991; Hegenberger, 1993; Hoffmann and Prave, 1996). They range from thin, allodapic, deep-water deposits (Kennedy, 1996), through agitated shelfal facies (James *et al.*, 2001), near-shore grainstones and stromatolites (Spencer and Spencer, 1972; Corkeron and George, 2001), to supratidal tepee beccias (Fig. 5g; Deynoux and Trompette, 1976). ‘Cap-carbonate sequences’ (see below and Fig. 3) share a distinct set of unusual sedimentary structures (Cloud *et al.*, 1974; Peryt *et al.*, 1990; Aitken, 1991; Fairchild, 1993; Grotzinger and Knoll, 1995; Kennedy, 1996; Hoffman *et al.*, 1998a; James *et al.*, 2001), and they are consistently depleted in ^{13}C relative to other Neoproterozoic carbonates (Knoll and Walter, 1992; Kaufman and Knoll, 1995; Kaufman *et al.*, 1997; Hoffman

Terra Nova, Vol 14, No. 3, 129–155

et al., 1998b; Kennedy *et al.*, 1998; Myrow and Kaufman, 1999; Brasier and Shields, 2000; Walter *et al.*, 2000). They share certain features with Archean and some pre-Neoproterozoic carbonates (Grotzinger and Knoll, 1995; Grotzinger and James, 2000; Sumner, in press), but they are without parallel in the Phanerozoic. They have long been considered paradoxical because they suggest that an abrupt transformation from glacial to tropical conditions took place virtually everywhere (Spencer, 1971; Schermerhorn, 1974; Williams, 1979; Fairchild, 1993). Kirschvink (1992) did not foresee cap carbonates as consequential to snowball events – he was unaware of their existence (personal communication, 1999) – but they are a striking affirmation of the second testable implication (see above) of his theory. In cap carbonates, we see the 'smoke', if not the 'gun', of the snowball Earth.

'Cap dolostones' (Fig. 3) are the transgressive systems tracts (Van Wagoner *et al.*, 1988) of depositional sequences ('cap-carbonate sequences') associated with post-glacial sea-level rise. They typically grade across a marine flooding surface (Fig. 3) into deeper water limestone or shale, which gradually shoals upward through carbonate or siliciclastic lutites and arenites to an exposure surface 100s of metres above the base of the sequence (Figs 4a and 9). The great thickness and deep-water aspect of many cap-carbonate sequences (von der Borch *et al.*, 1988; Narbonne and Aitken, 1995; Dalrymple and Narbonne, 1996; Hoffman *et al.*, 1998b) is anomalous within their overall stratigraphic context (Fig. 9). This is commonly ascribed to post-glacial sea-level rise, but long-term tectonic subsidence is required to preserve the sequence from isostatically driven erosion, because the glacio-eustatic cycle alone creates no permanent accommodation space. On the Otavi carbonate platform in northern Namibia, an estimated background tectonic subsidence rate equivalent to ~ 0.065 mm yr^{-1} of isostatically adjusted carbonate (Halverson *et al.*, 2002) implies a timescale on the order of 5 million years to create the accommodation space occupied by the younger cap carbonate sequence (Fig. 9), which is 300–400 m thick. Hoffman *et al.* (1998a) suggested that that the snowball event occupied the vast majority of this time, when the average sedimentation rate on the platform was very low. By the end of the event, substantial net subsidence had occurred, although masked at that time by relative sea-level fall. Upon deglaciation, sea level rose and chemical and/or detrital sediments rapidly filled in the accommodation space provided, making up for 'lost time', so to speak. High sedimentation rates in cap dolostones and overlying limestones are consistent with their low δ^{13}C values (see above) and with their petrological characteristics (see below).

Petrologists, being fascinated by the unusual, have had a field day with cap carbonates (Peryt *et al.*, 1990; Aitken, 1991; Fairchild, 1993; Grotzinger and Knoll, 1995; Kennedy, 1996; Hoffman *et al.*, 1998b; James *et al.*, 2001; Kennedy *et al.*, 2001a; Corsetti and Kaufman in press; Sumner, in press). The Elatina, Ghaub, Ice Brook, Landrigan and Numees glacial deposits (Table 1) are directly overlain by pale, flinty, very pure, cap dolostones (Fig. 3), generally 3–30 m thick (Aitken, 1991; Kennedy, 1996; James *et al.*, 2001). They are invariably well laminated and, at proper palaeodepths, hummocky cross-laminated with laminae defined by sets of reverse-graded peloids (Fig. 4b) (Aitken, 1991; Kennedy, 1996; James *et al.*, 2001). Structures referred to as 'tepees' (Fig. 4c) occur in all the above but they have neither the geometry nor associations of conventional supratidal tepees (Kendall and Warren, 1987). In plan, they are linear and parallel, orientated subparallel to the regional palaeoslope (Williams, 1979; Eisbacher, 1981; Aitken, 1991; Kennedy, 1996; James *et al.*, 2001), not polygonal like conventional tepees (Fig. 5g), which result from lateral expansion due to the force of crystallization (Kendall and Warren, 1987). Inspection of their cuspate axial zones (Fig. 4d) reveals that they formed by continuous aggradation in a highly oscillatory flow regime. Microbial bioherms (Fig. 5a–c) and biostromes (stromatolites) occur within some cap dolostones (Spencer and Spencer, 1972; Cloud *et al.*, 1974; Wright *et al.*, 1978; Walter and Bauld, 1983; Bertrand-Sarfati *et al.*, 1997; Hoffman *et al.*, 1998a; Corkeron and George, 2001; James *et al.*, 2001). In Namibia and the North American Cordillera, stromatolites in cap dolostones of the Ghaub, Numees (and correlative Bildah), Wildrose, and Ice Brook glaciations (Table 1) are distinguished by internal, vertically orientated, tube-like or sheet-like pockets of infilled micritic sediment and cement (Cloud *et al.*, 1974; Hegenberger, 1987, 1993; Hoffman *et al.*, 1998a, 2002a). The tube-like variety (Fig. 5b) has been attributed to gas escape (Cloud *et al.*, 1974; Hegenberger, 1987; Kennedy *et al.*, 2001a), but close inspection of well-preserved examples (Fig. 5c) reveals a stromatolitic (microbial) origin (Hoffman *et al.*, 1998a, 2002a; James *et al.*, 2001). The micritic sediment gathered in shallow pits or gutters on the stromatolitic surface, which aggraded with remarkably little change in morphology (Fig. 5b). As a result, the sediment-filled pits and gutters became vertical tubes and sheets, respectively. The pitted stromatolite surfaces must have resembled giant golf balls (so designed to reduce drag). Cap dolostones have much more to reveal (Hoffman *et al.*, 2002b), but the whole ensemble of structures suggests rapid aggradation on storm-dominated ramps.

Locally, cap dolostones are overlain by limestone buildups composed largely of sea-floor cements (Peryt *et al.*, 1990; Aitken, 1991; Grotzinger and Knoll, 1995; Kennedy, 1996; Soffer, 1998; James *et al.*, 2001). The cements consist of upward-fanning, prismatic crystals pseudomorphosed by calcite (Figs 4f and 5e). The square-tipped, pseudo-hexagonal habit of the crystals indicates that the primary phase was aragonite. Although individual crystal fans are small (< 1 cm), they aggregate into reef-like masses (pseudo-stromatolites) that range from metres to decametres in scale (Fig. 5a,d). The cements did not precipitate slowly in the absence of particulate sediment, but grew rapidly in a race against micritic burial (Figs 4f and 5d,e). The cementstone buildups are up to 50 m thick, but eventually they give way to flaggy, allodapic, pink limestone with large-scale hummocky cross-bedding (Maieberg Formation, Namibia), or to black, organic-rich shale (Sheepbed Formation, Canada). The cements imply a high degree of carbonate oversaturation (Grotzinger and Knoll, 1995; Sumner, in press) and the dendritic-prismatic growth habit suggests rapid, diffusion-limited, growth rates (Lasaga, 1998). The presence of dissolved Fe(II) may have inhibited carbonate nucleation in anoxic waters below the mixed layer, thereby promoting the growth of crystal fans on the sea floor (Sumner and Grotzinger, 1996) while the micritic component nucleated in oxic surface waters. Deep-water anoxia is inevitable if the ocean was ice-covered for long periods (see below) and is consistent with dolomitization of cap dolostones on the sea floor (Baker and Kastner, 1981) and with the co-occurrence of sea-floor barite precipitates (Fig. 4e). The localization of these cementstone buildups at ancient shelf breaks (Soffer, 1998; James *et al.*, 2001) suggests that their occurrence may be dictated by upwellings.

Differences among cap-carbonate sequences have elicited debate as to temporal vs. spatial control (Kennedy *et al.* 1998; Brasier and Shields, 2000). Some examples (Fig. 3d,e) lack transgressive systems tracts and their isotopic profiles also appear base truncated – the descending phase of the δ^{13}C anomaly is missing (Hoffman *et al.*, 2001). This could result from undersaturation of the local water mass until after the post-glacial sea-level rise was complete, bearing in mind the large alkalinity input required to maintain saturation if atmospheric pCO$_2$ rose to high levels (Fig. 10) during the hypothesized snowball event. Base truncation appears more typical of 'Sturtian' (Table 1) cap-carbonate sequences (Kennedy *et al.*, 1998), and could mean that the glacial ocean was less well buffered by carbonate dissolution and/or that less carbonate was available for weathering during deglaciation (see below). While actively subsiding areas (Kimberley, Adelaide, Cordillera, Otavi) have thick (200–1200 m) post-glacial sequences (Plumb, 1981; von der Borch *et al.*, 1988; Christie-Blick *et al.*, 1995; Narbonne and Aitken, 1995; Hoffman *et al.*, 1998a), the Jbéliat cap-carbonate sequence in the cratonic Taoudeni basin (Deynoux and Trompette, 1976) is highly condensed (Figs 3 and 11). After isostatic adjustments, minimal accommodation space remained after post-glacial sea-level rise because the background tectonic subsidence rate was very low. The cap carbonate built rapidly to sea level, resulting in the formation of spectacular supratidal tepee structures (Fig. 5g) and associated, early diagenetic (phreatic), barite crusts (Fig. 5f). We speculate the latter may have formed in a meteoric-marine groundwater mixing zone beneath a surface exposed to the hypothesized transient greenhouse atmosphere. Where the sequence expands to fill palaeovalleys (Fig. 11), the transgressive nature of the basal cap dolostone which drapes the palaeotopography is apparent. The Jbéliat example is also interesting inasmuch as the glacial deposits (continental tillites and outwash) preceded the hypothesized snowball event, which is apparently represented by a regolith horizon (Fig. 11) with well-developed polygonal sand wedges (Deynoux, 1982, 1985). This horizon separates the glacial deposits from the cap dolostone, and marks a period when ablation exceeded precipitation in the region. Cap carbonates also thin basinward: the Maieberg Formation is 300–400 m thick on the Otavi platform (Fig. 9), but its equivalent (correlated isotopically) thins to < 25 m within 30 km downslope from the shelf break (Hoffman *et al.*, 1998b; Kennedy *et al.*, 1998).

We are not burdened by an overabundance of explanations for cap carbonates. Fairchild (1993) suggested that they were precipitated from glacial meltwaters saturated with alkalinity due to interaction with carbonate-rich glacial debris and rock powder. This does not adequately explain the presence of cap carbonates in areas where the glacial deposits have little carbonate, for example the Kimberleys in Australia (Plumb, 1981). Grotzinger and Knoll (1995) proposed that cap carbonates record the turnover of a previously stratified ocean (see above), with upwelling of alkalinity-laden deepwater driving precipitation of ^{13}C-depleted carbonates. This model dovetails with Kirschvink's (1992) post-glacial interpretation of Neoproterozoic BIF (Klein and Beukes, 1993), but the premise is questionable for reasons already given. Kennedy (1996) related cap carbonates to post-glacial flooding of continental shelves and seas, analogous to the 'coral reef' hypothesis for the Quaternary (Berger, 1982), and Kennedy *et al.* (2001a) hypothesized that cap carbonates are byproducts of methane released from permafrost on continental shelves globally during post-glacial flooding. But methane oxidized aerobically in the water column produces CO$_2$, causing carbonate dissolution; only methane oxidized anaerobically in conjunction with bacterial sulphate reduction in pore waters yields bicarbonate (Boetius *et al.*, 2000). If very large amounts of methane were released rapidly (Kennedy *et al.*, 2001a), sulphate limitaton would likely prevent substantially increased rates of anaerobic methane oxidation. Moreover, the characteristic spatial variability in $\delta^{13}C_{carb}$ (− 40 to 0‰) observed in Phanerozoic methane-seep carbonates (Kauffman *et al.*, 1996) is not found in cap carbonates. Tube-like structures purportedly conduits for methane release (Kennedy *et al.*, 2001a) are strictly internal to cap carbonates (Fig. 5b): they do not tap the conjectured methane source rocks (Hoffman *et al.*, 2002a). They occur only within microbial boundstones (Fig. 5c), even in cap dolostones deposited directly on metamorphic or granitic rocks (Cloud *et al.*, 1974; Wright *et al.*, 1978), unlikely to be prolific sources of methane.

Once we realized that the snowball hypothesis could explain the δ^{13}C anomalies associated with LNGD, we took as a test that it should also account for cap carbonates. Recall the deglaciation of a snowball Earth, sea ice and glaciers disappearing rapidly due to reverse ice-albedo feedback in an intense greenhouse with > 10% CO$_2$ (Caldeira and Kasting, 1992). As surface temperatures soar, carbonic (and initially sulphuric) acid rain beats down on a landscape dominated by frost-shattered rock and rock powder from glacial action, not to mention millions of years' worth of unaltered volcanic material (Hoffman *et al.*, 1998b; Hoffman and Schrag, 2000). Intense chemical (and physical) weathering ensues. Initially, where former carbonate platforms are exposed, carbonate weathering dominates. Later, after sea level has risen, silicate weathering becomes proportionally more important, and over time, draws down the atmospheric

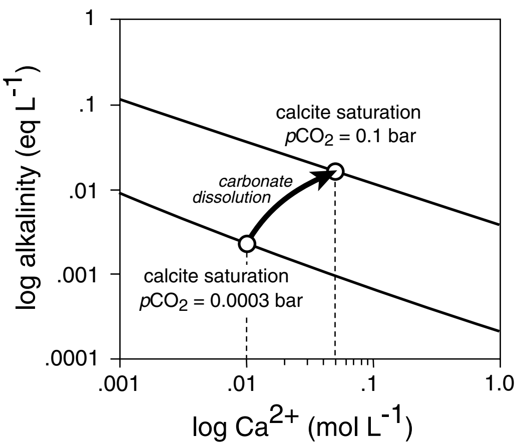

Fig. 10 Alkalinity as a function of Ca ion concentration for seawater at saturation with respect to $CaCO_3$ in equilibrium with an atmospheric $pCO_2 = 0.0003$ bar (i.e. onset of snowball event) and $pCO_2 = 0.1$ bar (i.e. aftermath of snowball event). Note five-fold increase in Ca ion concentration required to maintain saturation over the course of a hypothesized snowball event.

CO_2 until a new steady state is reached (Hoffman and Schrag, 2000). The time scale of the greenhouse transient is unknown, but is conservatively estimated to be in the range 10^4–10^6 years [not $< 10^4$ years as suggested by Kennedy *et al.* (2001b)]. The alkalinity flux driving cap carbonate deposition during post-glacial sea level rise (i.e. below 'maximum flooding' in Figs 3, 9) came from carbonate weathering; silicate weathering is too slow, given a deglaciation time of $< 10^4$ years (Kennedy *et al.*, 2001b).

Large inputs of alkalinity are required to maintain seawater saturation if atmospheric pCO_2 greatly increased in a snowball event (Fig. 10). The hydrothermal dominance of the snowball ocean will drive down seawater pH unless it is buffered by dissolution of carbonate, supplied for example by glacial action. Buffering would enable cap carbonates to form immediately upon deglaciation. This is consistent with the inference (see above) that many cap carbonates formed during post-glacial transgression (Fig. 3) and with the absence of post-glacial karst beneath cap carbonates. The deglaciation of a snowball Earth involves the rapid generation and mixing of warm, oxic, surface water with cold, saline deepwater, the latter dominated hydrothermally and the former by melting and runoff that is alkalinity-laden from carbonate weathering. The internal stratigraphy of complex cap carbonates may reflect, in addition to changing water depth, the mixing of contrasting water masses (Hoffman *et al.*, 2002).

Test 3: iron formations

For Joe Kirschvink, iron is the element of choice. Iron formations are extensive deposits of sedimentary Fe(III) oxide and chert, not directly associated with volcanoes or hydrothermal vents. Common in the early stratigraphic record (Fig. 12), they virtually disappear after 1.85 Ga (Isley and Abbott, 1999). The only major reappearances of iron formation since that time (barring Clinton-type oolitic ironstones) occur strictly within LNGD (Fig. 2d), notably in Canada (Young, 1976; Yeo, 1981, 1986; Klein and Beukes, 1993), Brazil (Urban *et al.*, 1992; Graf *et al.*, 1994; Trompette *et al.*, 1998), Namibia–South Africa (Martin, 1965) and Australia (Preiss, 1987; Lottermoser and Ashley, 2000).

The prerequisites for iron formation are three (Drever, 1974; Holland, 1984): (1) ocean anoxia to allow extensive transport of dissolved Fe(II); (2) an H_2S:Fe(II) flux ratio < 2, so that not all Fe(II) is scavenged by sulphide (FeS_2) burial, and (3) a local oxidant to drive the precipitation of an iron-formation precursor. Before the first atmospheric oxidation event around 2.4 Ga (Karhu and Holland, 1996), deep waters were anoxic and riverine sulphate input was low (Walker and Brimblecombe, 1985; Canfield *et al.*, 2000; Farquhar *et al.*, 2000). After 2.4 Ga, deepwater anoxia arguably persisted, but not until 1.8 Ga did oxidative weathering drive sulphate reduction in the ocean to levels sufficient to bury all Fe(II) as FeS_2 (Canfield, 1998). The reappearance of iron formation in LNGD, after a 1.5-billion-year absence, is consistent with ocean anoxia due to stagnation beneath near-global sea-ice cover (Kirschvink, 1992), and also with an attenuated flux of reduced sulphur due to the frozen surface (Canfield and Raiswell, 1999).

Kirschvink (1992) and his early supporters (Klein and Beukes, 1993) suggested that Neoproterozoic iron formations were deposited at the end of snowball events, when renewed thermohaline circulation would have driven Fe(II)-rich deepwater into the oxic zone in upwelling areas. This model has been criticized on the grounds that iron formation occurs stratigraphically within or below, rather than above, certain LNGD (Williams and Schmidt, 2000). However, glacial erosion at low latitudes will itself be strongly biased toward the end of a snowball event, when the hydrological cycle has strengthened (Fig. 7). Alternatively, iron formation may have been deposited beneath the tropical ice pack if sea ice was thin (< 20 m) or discontinuous (McKay, 2000; but see Warren *et al.*, 2002). Oxygenic photosynthesis would drive precipitation, given an anoxic ocean rich in dissolved iron. The giant Rapitan iron formations in the northern Canadian Cordillera, for example, were deposited close to the equator (Park, 1997) and are overlain by < 600 m of glacial diamictite and outwash (Yeo, 1981). [Young (1988) attributes the Rapitan iron formation to regional (but cryptic), rift-related, hydrothermal activity, but this is not supported by its trace-element geochemistry (Klein and Beukes, 1993; Graf *et al.*, 1994) and ignores the complete absence of volcanics in the Rapitan belt and the age distribution of iron formations globally (Fig. 12).]

Kennedy *et al.* (1998) pointed out that iron formation is more common in (but not limited to) 'Sturtian'

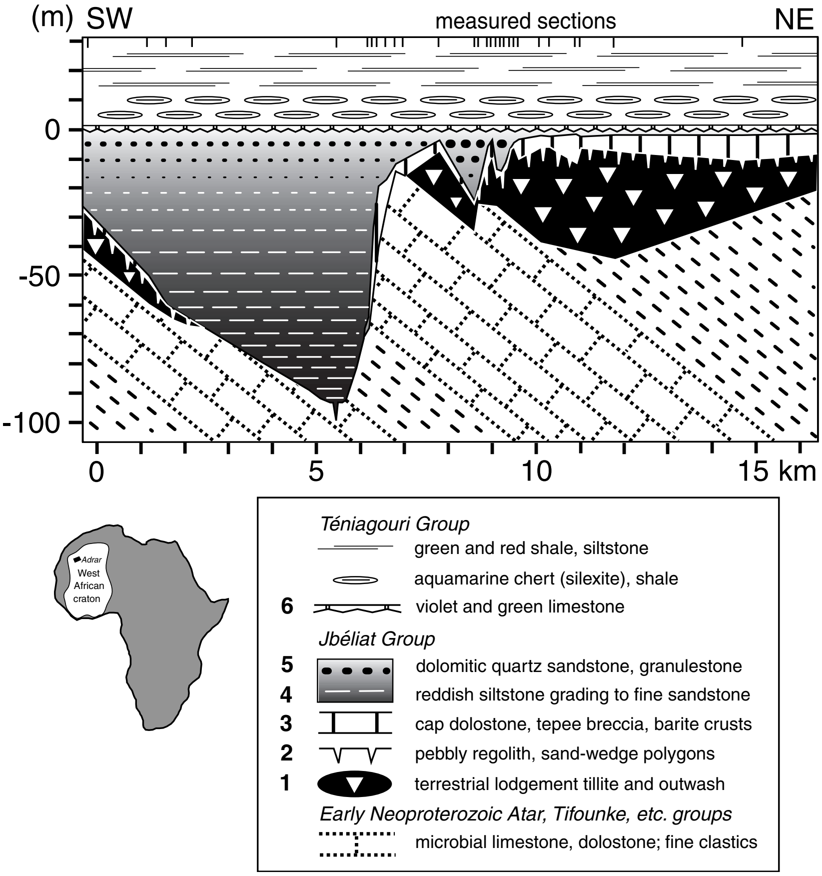

Fig. 11 Complex history of the cratonic Jbéliat glaciation (Table 1) and its aftermath inferred from stratigraphic sections measured by the senior author, G. P. Halverson and A. C. Maloof on the Atar Cliffs of Adrar, Mauritania (Deynoux, 1980). Sequence of events (see legend): 1 Deposition of terrestrial glacial deposits on tilted early Neoproterozoic strata. 2 Erosion of palaeovalley and subsequent development of permafrost regolith with polygonal sand wedges and deflation lag. 3 Post-glacial transgression with deposition of cap dolostone mantling topography. Intense diagenesis of cap dolostone outside palaeovalley due to subaerial exposure (beneath hypothesized greenhouse atmosphere) following isostatic adjustment. 4–5 Infilling of palaeovalley via side-valleys by coarsening-upward terrigenous sequence terminated at a dolomite-cemented exposure surface. 6 Transgression, with reworking and deposition of a limestone veneer, highly silicified mudrock (silexite) and shales of the Téniagouri Group. We tentatively interpret stage 2 as representing the hypothesized snowball event, implying that ablation exceeded precipitation during the snowball event itself and that the glacial deposits pre-date the ice-albedo runaway. Dominantly terrigenous late Neoproterozoic succession is consistent with a middle or high palaeolatitude, where glacial deposition should lead the ice-albedo runaway. Condensed nature of the sequence (outside palaeovalleys) is attributed to a low rate of ongoing tectonic subsidence in this cratonic basin.

glacial deposits (Table 1). A speculative explanation for this observation is the hydrostatic pressure dependence of the H_2S:Fe(II) ratio in hydrothermal vent fluids at mid-ocean ridges (Kump and Seyfried, 2001). A large fall of sea level would result in a lowering of this ratio, favouring BIF deposition (Kump and Seyfried, 2001). Many of the 'Sturtian' deposits occur in rift zones and they tend to be orders of magnitude thicker than the 'Varanger/Marinoan' deposits (Eisbacher, 1981; Miller, 1985; Preiss, 1987; Young and Gostin, 1991; Brookfield, 1994; Aleinikoff *et al.*, 1995; Narbonne and Aitken, 1995; Hoffman and Schrag, 1999). Arguably, there was more topography at low latitudes globally, giving rise to more massive ice sheets. This would have caused a larger sea-level fall and, according to Kump and Seyfried (2001), a greater propensity for iron formation.

Questioning the snowball Earth

The snowball hypothesis has properly been questioned and the sharpest questions to date concern the terrestrial glacial regime, the isotopic evolution of snowball seawater and the fate of eukaryotic organisms. These and other questions highlight the central difficulty with the hypothesis, which is our limited conception of a snowball event itself. With postulated conditions lying far outside familiar parameter space, there is danger that the hypothesis we question is a caricature of a snowball Earth.

Would glaciers flow?

Geological evidence for the existence of dynamic glaciers is incontrovertable. Many LNGD contain faceted and striated clasts (Fig. 2b), some far-travelled, and deformation structures caused by glacial flow (Cahen, 1963; Eisbacher, 1981; Wang *et al.*, 1981; Edwards, 1984; Deynoux, 1985; McMechan, 2000). Associated subglacial pavements (Fig. 2a) are indelibly shaped, scratched, cracked and polished by glacial motion (Reusch, 1891; Perry and Roberts, 1968; Deynoux, 1980; Rice and Hofmann, 2000). Are these observations compatible with the cold, dry atmosphere and limited hydrological cycle of a snowball Earth (Christie-Blick *et al.*, 1999; McMechan, 2000)? A major difficulty with this question is that we do not generally know which phase of the glacial cycle (Fig. 7) the glacial deposits represent. The magnetic reversal record in the Elatina (Sohl *et al.*, 1999), however, indicates that a significant part of the hypothesized snowball event is represented.

Climate models suggest that an ice-albedo runaway might occur very rapidly (Hyde *et al.*, 2000), freezing the tropical oceans before ice sheets had time to develop on low-latitude continents (Hoffman *et al.*, 1998b; Pollard and Kasting, 2001). During a snowball event, mean temperatures slowly rise (Fig. 7) in response to atmospheric CO_2 and this will cause an exponential increase in saturation

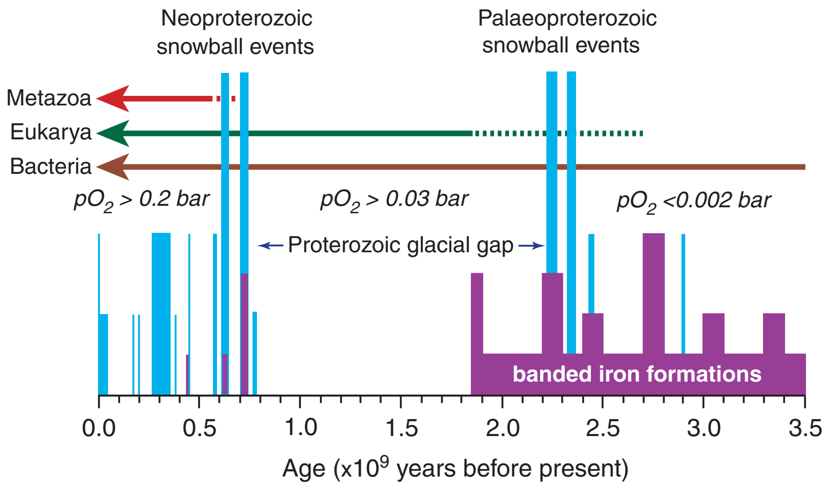

Fig. 12 Frequency of occurrence of iron formations (purple) (modified from Isley and Abbott, 1999), major glacial periods (blue) (Crowell, 1999), constraints on atmospheric oxygen levels (Rye and Holland, 1998), and steps in the history of life. Note the two eras of snowball events separated by a 1.5 billion year gap when evidence is lacking for glaciation at any latitude.

vapour pressures. Moisture sources include subaerial volcanic outgassing, sublimation of tropical sea ice (Warren *et al*., 2002), and evaporation of transient melt ponds (Walker, 2001) and polynyas within the tropical ice pack (Kirschvink, 1992). Given large seasonal and diurnal fluctuations in surface temperature (Walker, 2001), water vapour would be advected to topographic highs on summer afternoons and moisture would condense there forming glaciers (Walker, 2001). Due to the weak hydrological cycle, snow accumulation rates would be extremely low, but a positive feedback would develop between surface elevation and snow accumulation if glaciers thickened. Over sufficient time, these glaciers must become wet-based and flow, possibly in localized ice streams or as episodic ice surges (Bentley, 1987; MacAyeal, 1993). The observed zonal distribution of LNGD (Fig. 1) might broadly reflect the zonal pattern of precipitation minus ablation on the snowball Earth. On the regional scale, the importance of topography, particularly coastal topography, in capturing the limited precipitation is not inconsistent with the common observation that thicker glacial deposits occur in tectonically more active areas and times (Young, 1995). They commonly overlie preglacial strata with angular unconformity, consistent with a prolonged hiatus (with ongoing block rotation) between the ice-albedo runaway and the onset of glacigenic sedimentation (Fig. 7). Where LNGD are absent, without evidence for removal by erosion, or where their position is occupied by aeolianite (Deynoux *et al*., 1989; Moussine-Pouchkine and Bertrand-Sarfati, 1997; Williams, 1998; Fig. 5a), ablation evidently exceeded precipitation over the full glacial cycle.

Would seawater change?

The elemental and isotopic composition of seawater should change in a snowball event. Decimated organic productivity and hydrothermal dominance should cause $\delta^{13}C$ and $^{87}Sr/^{86}Sr$, respectively, to fall (Kump, 1991; Jacobsen and Kaufman, 1999). The trajectories of the changes depend on the C and Sr residence times, and are sensitive to buffering by carbonate dissolution (Jacobsen and Kaufman, 1999) in response to submarine volcanic exhalations of CO_2 and other acids. Consequently, few $\delta^{13}C$ or $^{87}Sr/^{86}Sr$ values have been reported for the glacial ocean because primary synglacial carbonates are rare. Kennedy *et al*. (2001b) report positive $\delta^{13}C$ values from purported examples in Australia, Namibia and California, whereas Xiao *et al*. (2001) find that thin calcareous crusts in the Tereeken glacials (Table 1) of NW China have $\delta^{13}C$ close to − 5‰.

Cap carbonates have been substituted as proxies for seawater $^{87}Sr/^{86}Sr$ during snowball events (Jacobsen and Kaufman, 1999; Kennedy *et al*., 2001b), justified by the Sr residence time of ~ 3.5 Myr in the present ocean. Neoproterozoic Sr isotope data are not very reliable because strontium is a mobile trace element and most carbonates of that age are totally recrystallized (Derry *et al*., 1992). Nevertheless, the 'least altered' $^{87}Sr/^{86}Sr$ ratios in cap limestones (dolomites have very low Sr concentrations) are not significantly different from preglacial values (Jacobsen and Kaufman, 1999; Kennedy *et al*., 2001b). This may be interpreted in two ways. Either the $^{87}Sr/^{86}Sr$ ratio of seawater changed little because the glaciation was short-lived (Jacobsen and Kaufman, 1999), contrary to palaeomagnetic (Sohl *et al*., 1999) and subsidence (Hoffman *et al*., 1998a) data, or else the ratio was buffered by carbonate dissolution during the hypothesized snowball event and enhanced weathering in the greenhouse aftermath (Hoffman *et al*., 1998b). If atmospheric pCO_2 rose from a preglacial value of 0.0003 bar to 0.12 bar over the course of a snowball event (Caldeira and Kasting, 1992), then the Ca ion concentration of seawater would have to increase five-fold simply to maintain carbonate saturation (Fig. 10). This enormous Ca input would be accompanied by a flux of isotopically conservative Sr from carbonate dissolution and radiogenic Sr from silicate weathering. These inputs might greatly reduce or even eliminate the predicted lowering of $^{87}Sr/^{86}Sr$ during a snowball event of any given duration (Jacobsen and Kaufman, 1999). The large magnitude of the resulting seawater Sr reservoir, plus the rapid weathering of carbonates and young volcanics, would damp any increase in seawater $^{87}Sr/^{86}Sr$ due to silicate weathering, consistent with available data (Jacobsen and Kaufman, 1999; Kennedy *et al*., 2001b). Contrary to Kennedy *et al*. (2001b), the transient weathering flux is not limited to the time-scale of the sea-level rise (< 10^4 years) but continued long after as indicated by the negative $\delta^{13}C$ anomaly (Fig. 9) which encompasses the entire transgressive–

regressive post-glacial sequence. Accordingly, $^{87}Sr/^{86}Sr$ ratios in cap carbonates are broadly similar to preglacial values but should rise there-after due to silicate weathering, as is observed (Shields *et al*., 1997).

Would eukoryotes survive?

Few biologists doubt that prokaryotic organisms could survive snowball events (Priscu *et al*., 1998; Gaidos *et al*., 1999; Vincent and Howard-Williams, 2000; Thomas and Dieckmann, 2002), but many extant clades of eukaryotic algae, protists and testate amoebae are known from earlier strata (Butterfield *et al*., 1990, 1994; German, 1990; Butterfield and Rainbird, 1998; Butterfield, 2000; Porter and Knoll, 2000) and they must have prevailed as well. A marked decline in eukaryotic and total microfloral diversity occurred around the time of the LNGD (Vidal and Knoll, 1982; Schopf, 1991; Knoll, 1994; Vidal and Moczydlowska-Vidal, 1997) and it is not until well after the Elatina/Nantuo glaciation (Table 1) that an abrupt increase in abundance, size, morphological complexity, and taxonomic diversity of acanthomorph acritarchs is observed (Zhang *et al*., 1998; Grey, 1998; Walter *et al*., 2000). The enigmatic, soft-bodied, Ediacara macrofossils – arguably dominated by cnidarian-grade metazoans – appears world-wide by 575–555 Ma (Fedonkin, 1992; Jenkins, 1992; Seilacher, 1992; Fedonkin and Waggoner, 1997; Knoll and Carroll, 1999; Martin *et al*., 2000). In north-western Canada, simple Ediacara-type fossils with radial symmetry occur in the immediate post-glacial sequences of both the Rapitan (Hofmann *et al*., 1990) and Ice Brook (Narbonne and Aitken, 1990; Narbonne, 1994) glaciations (Table 1). Most molecular-based estimates of bilaterian radiations pre-date the hypothesized snowball events (Runnegar, 2000), but there are good reasons to take these estimates lightly (Peterson and Takacs, 2001).

Assuming snowball events occurred, what refugia ensured the survival of eukaryotic plankton, and early metazoans if they existed? How did the climate shocks entering and exiting snowball events impact their evolution? A variety of refugia would have existed and their relative isolation and selective stresses could have contributed to evolutionary diversification. They include brine channels in new sea ice (Thomas and Dieckmann, 2002), polynyas in the tropical ice pack (Kirschvink, 1992; Lemke, 2001), tidal cracks along ice-grounding lines (Gaidos *et al*., 1999), transient meltwater ponds (Walker, 2001), beneath clear sea or lake ice < 20 m thick (McKay, 2000), and shallow hot springs around volcanic islands (Hoffman and Schrag, 2000). Snowball seawater would be laden with nutrients due to hydrothermal activity and limited organic productivity (Kirschvink *et al*., 2000) particularly in the younger Neoproterozoic glaciations when iron formation, a major sink for phophorus, was rare (see above). Enhanced productivity and burial of organic matter when snowball oceans were uncorked would have released oxygen to the atmosphere (Kirschvink *et al*., 2000; Walter *et al*., 2000), consistent with evidence of increased environmental oxygenation roughly coincident with the Palaeoproterozoic (Prasad and Roscoe, 1996; Rye and Holland, 1998; Farquhar *et al*., 2000; Murakami *et al*., 2001) and Neoproterozoic (Des Marais *et al*., 1992; Logan *et al*., 1995; Canfield and Teske, 1996) snowball eras (Fig. 12). The isotopic signal of such organic-burial events might be muted if they were accompanied by a high carbonate burial flux, driven by weathering as we have argued. The appearance of particular Ediacaran fossils has long been attributed to a rise in free oxygen (Runnegar, 1982; Knoll and Carroll, 1999). Speculatively, snowball events may have acted not only as an environmental filter on the evolution of life, but also as a biogeochemical pump that permanently changed the environment itself.

Snowball events in Earth history

Any viable explanation for snowball events must also explain why they are rare. Extensive low-latitude glaciation occurred only near the beginning (2.45–2.22 Ga) and the end (0.73–0.58 Ga) of the Proterozoic eon (Fig. 12). The former include the Makganyene glacials in South Africa (Evans *et al*., 1997; Tsikos and Moore, 1998; Kirschvink *et al*., 2000), three discrete Huronian glaciations in central Canada (Williams and Schmidt, 1997; Schmidt and Williams, 1999), and equivalents in Wyoming and Finland (Ojakangas, 1988). The Makganyene and Huronian glacials have similar age brackets, > 2.22 and < 2.45 Ga (see references in Williams and Schmidt, 1997; Bekker *et al*., 2001). The Makganeyene glaciation was preceded by carbonates with unusually high $\delta^{13}C$ values, similar to LNGD (Bekker *et al*., 2001), and succeeded by a major Fe–Mn sedimentary formation (Tsikos and Moore, 1998; Kirschvink *et al*., 2000). The middle Huronian and equivalent glacial units have cap carbonates (the only carbonate in the 14-km-thick Huronian succession) with negative $\delta^{13}C$ (Veizer *et al*., 1992; Bekker *et al*., 2001), and the ultimate Huronian glaciation was followed by an intense lateritic weathering regime (Young, 1973). Remarkably, there is virtually no evidence for large ice sheets at any palaeolatitude during the 1.5 billion years in between the two snowball eras (Fig. 12). Two things need to be explained (Schrag *et al*., 2002): what special conditions set those two eras apart (allowing snowball events to occur), and what triggered the individual snowball events?

The length of both eras, 100–200 Myr, is of the time-scale of global palaeogeographical reorganizations due to plate tectonics. Kirschvink (1992) proposed that a preponderance of land masses in the middle and low latitudes set the stage for snowball events, consistent with existing palaeomagnetic data for LNGD (Fig. 1). This is broadly in line with global reconstructions for 750 Ma (Fig. 7), prior to the 'Sturtian' (Table 1) glaciation(s), but 'Varanger–Marinoan' (Table 1) palaeogeography is quite uncertain, primarily because of poor age control. Reconstructions in which land masses are centred on the (south) pole (e.g. Hyde *et al*., 2000; Baum and Crowley, 2001; Crowley *et al*., 2001) hinge on Laurentia's migration to high latitudes by 577 Ma (Torsvik *et al*., 1996), after the last snowball event (Table 1), a migration which could have ended the snowball era rather than being a precondition for it (Hyde *et al*., 2000). Placing continents at tangent to the tropics results in a colder Earth for a variety of reasons.

It raises the surface albedo (Kirschvink, 1992) and it enhances silicate weathering, unless tectonic activity is mysteriously absent there (Marshall *et al*., 1988; Worsley and Kidder, 1991; Schrag *et al*., 2002). Weathering rates are greater on small continents because they are wetter than large ones. The Neoproterozoic snowball era was a period of continental dispersal, involving the breakup of supercontinent Rodinia and the aggregation of megacontinent Gondwana (Hoffman, 1999). Polar ice caps may reduce global weathering rates and mitigate against snowball events if large land areas exist at high latitudes (Schrag *et al*., 2002), as in the Phanerozoic. An absence of high-latitude continents and a preponderance of tropical and subtropical land masses would be an unusual situation in Earth history, and might give rise to polar sea-ice caps large enough to threaten runaway ice-albedo feedback (Kirschvink, 1992; Schrag *et al*., 2002).

Clues regarding the triggering of individual snowball events may be found in preglacial $\delta^{13}C$ records (Figs 8 and 9). Snowball events generally follow long stages ($> 10^7$ years) of high $\delta^{13}C$ ($> 5‰$ PDB in shallow marine carbonates) (Kaufman *et al*., 1997; Brasier and Shields, 2000; Walter *et al*., 2000; Halverson *et al*., 2002). This likely signifies that organic matter was disproportionately represented in the global carbon burial flux ($f_{org} \geq 0.4$). We speculate (Schrag *et al*., 2002) that a preponderance of middle- and low-latitude continents would produce this effect. Nutrient transport patterns will cause marine biological productivity to be focused in the congested middle and low latitudes where high rates of organic production will drive some basins to become anoxic (Schrag *et al*., 2002). Anoxic bottom waters cause high C:P ratios in the organic burial flux (Van Cappellen and Ingall, 1994; Colman and Holland, 2000), which greatly increases phosphorus availability for recycling, which in turn allows high sustained rates of organic production and burial.

Spectacular declines in $\delta^{13}C$ (Figs 8 and 9) have been discovered directly beneath the younger LNGD in north-west Canada (Narbonne and Aitken, 1995), north-west Namibia (Hoffman *et al*., 1998b; Halverson *et al*., 2002), South Australia (Walter *et al*., 2000; McKirdy *et al*., 2001) and north-west China (Xiao *et al*., 2001), and also beneath the older LNGD in Scotland (Brasier and Shields, 2000) and north-east Svalbard (Halverson and Maloof, 2001). The time-scale of the isotopic anomaly in Namibia is estimated to be on the order of 0.5 Myr (Halverson *et al*., 2002). We argue that this anomaly is most likely the result of a sustained release of ^{12}C-enriched carbon, possibly methane generated in the organic-rich sediments previously deposited (Halverson *et al*., 2002; Schrag *et al*., 2002). A prolonged release of methane into the atmosphere, engendered by the unusual continental distribution, would not only drive down marine $\delta^{13}C$ but might also destabilize the climate. Because atmospheric methane is not equilibrated with the ocean, as is CO_2, any substantial dependence on methane greenhouse could counter-intuitively trigger a snowball event if the methane supply was interrupted for any reason (Pavlov *et al*., 2000; Schrag *et al*., 2002). These ideas are highly speculative and it remains to be seen if any or all snowball events were initiated in this way. Perhaps each event was triggered differently, a possibility that highlights the glaring uncertainty regarding the number and correlation of LNGD (Kaufman *et al*., 1997; Grey and Corkeron, 1998; Kennedy *et al*., 1998; Saylor *et al*., 1998; Prave, 1999b; Brasier and Shields, 2000; Walter *et al*., 2000; Corsetti and Kaufman, in press).

Conclusions

The appeal of the snowball hypothesis (Kirschvink, 1992) is that it provides credible explanations for many previously enigmatic features of Neoproterozoic Earth history. It explains: (1) the widespread distribution of LNGD on virtually every continent; (2) the palaeomagnetic evidence that glacial ice lines reached sea level close to the equator for long periods; (3) the stratigraphic evidence that glacial events began and ended abruptly; (4) the reappearance of iron formations, exclusively within glacial units, after an absence of 1.2 billion years; (5) the world-wide occurrence of cap carbonates with unusual features, resting sharply above successive LNGD; (6) the existence of very large positive and negative $\delta^{13}C$ anomalies, before and after each glacial event, respectively. The alternative 'loophole' model (Hyde *et al*., 2000; Runnegar, 2000) compromises many of these explanations (Schrag and Hoffman, 2001), and is therefore less attractive. As the observations have no parallel in the Phanerozoic, it should not be surprising that the events responsible for them have no Phanerozoic counterparts.

Following Kirschvink (1992), we speculate that a preponderance of continents in middle to low latitudes created conditions favourable for snowball events. Such conditions would be rarely met in Earth history overall, but could persist for intervals long enough to engender repeated snowball events, as is observed. A possible trigger for individual snowball events, suggested by carbon isotopic data in many areas (Halverson *et al*., 2002), arises counter-intuitively from a dependence on greenhouse methane, engendered by the same unusual continental distribution (Schrag *et al*., 2002).

Acknowledgments

We are grateful to A. Kröner and M. Schidlowski for inviting this paper, which stems from a 10-year study of Neoproterozoic successions, principally in Namibia, funded by the Tectonics, Earth System History, and Arctic programmes of the National Science Foundation (USA), and the Astrobiology Institute of the National Aeronautics and Space Administration (NASA). The Canadian Institute for Advanced Research, the Geological Surveys of Namibia and Morocco, the Norwegian Polar Institute, and Harvard University also supported this work. We thank G. P. Halverson, Hu Guowei, A. J. Kaufman, A. C. Maloof, A. R. Prave, G. Soffer, A. van Dusen and many others for field contributions, and G. P. Halverson and A. van Dusen for the new isotopic data presented here. We thank F. A. Carselti, J. L. Kirschvink, J. C. G. Walker, and S. G. Warren for comments and preprints.

References

Aitken, J.D., 1991. The Ice Brook Formation and Post-Rapitan, Late Proterozoic glaciation, Mackenzie Mountains, Northwest Territories. *Geol. Surv. Can. Bull*., **404**.

Aleinikoff, J.N., Zartman, R.E., Walter, M., Rankin, D.W., Lyttle, P.T. and Burton, W.C., 1995. U–Pb ages of metarhyolites of the Catoctin and Mount Rogers formations, central and southern Appalachians: evidence for two pulses of Iapetan rifting. *Am. J. Sci.*, **295**, 428–454.

Baker, P.A. and Kastner, M., 1981. Constraints on the formation of sedimentary dolomite. *Science*, **213**, 214–216.

Baum, S.K. and Crowley, T.J., 2001. GCM response to Late Precambrian ($\sim$ 590 Ma) ice-covered continents. *Geophys. Res. Lett.*, **28**, 583–586.

Bekker, A., Kaufman, A.J., Karhu, J.A., Beukes, N.J., Swart, Q.D., Coetzee, L.L. and Eriksson, K.A., 2001. Chemostratigraphy of the Paleoproterozoic Duitschland Formation, South Africa: implications for coupled climate change and carbon cycling. *Am. J. Sci.*, **301**, 261–285.

Bentley, C.R., 1987. Antarctic ice streams: a review. *J. Geophys. Res.*, **92**, 8843–8858.

Berger, W.H., 1982. Increase of carbon dioxide in the atmosphere during deglaciation: the coral reef hypothesis. *Naturwissenschaften*, **69**, 87–88.

Bertrand-Sarfati, J., Flicoteaux, R., Moussine-Pouchkine, A. and Ait Kaci Ahmed, A., 1997. Lower Cambrian apatitic stromatolites and phospharenites related to the glacio-eustatic cratonic rebound (Sahara, Algeria). *J. Sed. Res.*, **67**, 957–974.

Bidgood, D.E.T. and Harland, W.B., 1961. Palaeomagnetism in some East Greenland sedimentary rocks. *Nature*, **189**, 633–634.

Bloxham, J., 2000. Sensitivity of the geomagnetic axial dipole to thermal core–mantle interactions. *Nature*, **405**, 63–65.

Boetius, A., Ravenschlag, K., Schubert, C.J., Rickert, D., Widdel, F., Giesecke, A., Amann, R., Jørgensen, B.B. and Pfannkuche, O., 2000. A marine microbial consortium apparently mediating anaerobia oxidation of methane. *Nature*, **407**, 623–626.

Brasier, M.D. and Lindsay, J.F., 1998. A billion years of environmental stability and the emergence of eukaryotes: new data from northern Australia. *Geology*, **26**, 555–558.

Brasier, M., McCarron, G., Tucker, R., Leather, J., Allen, P. and Shields, G., 2000. New U–Pb zircon dates for the Neoproterozoic Ghubrah glaciation and for the top of the Huqf Supergroup, Oman. *Geology*, **28**, 175–178.

Brasier, M.D. and Shields, G., 2000. Neoproterozoic chemostratigraphy and correlation of the Port Askaig glaciation, Dalradian Supergroup of Scotland. *J. Geol. Soc. Lond.*, **157**, 909–914.

Brookfield, M.E., 1994. Problems in applying preservation, facies and sequence models to Sinian (Neoproterozoic) glacial sequences in Australia and Asia. *Precambrian Res.*, **70**, 113–143.

Budyko, M.I., 1966. Polar ice and climate. In: *Proceedings of the Symposium on the Arctic Heat Budget and Atmospheric Circulation* (J.O.Fletcher, ed.), pp. 3–21. The Rand Corp., Santa Monica, CA.

Budyko, M.I., 1969. The effect of solar radiation variations on the climate of the Earth. *Tellus*, **21**, 611–619.

Butterfield, N.J., 2000. Bangiomorpha pubescens n. gen., n. sp.: implications for the evolution of sex, multicellularity, and the Mesoproterozoic/Neoproterozoic radiation of eukaryotes. *Paleobiology*, **26**, 386–404.

Butterfield, N.J., Knoll, A.H. and Swett, K., 1990. A bangiophyte red alga from the Proterozoic of arctic Canada. *Science*, **250**, 104–107.

Butterfield, N.J., Knoll, A.H. and Swett, K., 1994. Paleobiology of the Neoproterozoic Svanbergfjellet Formation, Spitsbergen. *Fossils Strata*, **34**, 1–84.

Butterfield, N.J. and Rainbird, R.H., 1998. Diverse organic-walled fossils, including 'possible dinoflagellates', from early Neoproterozoic of arctic Canada. *Geology*, **26**, 963–966.

Cahen, L., 1963. Glaciations anciennes et dérive des continents. *Ann. Soc. Geol. Belg.*, **86**, 19–83.

Caldeira, K. and Kasting, J.F., 1992. Susceptibility of the early Earth to irreversible glaciation caused by carbon dioxide clouds. *Nature*, **359**, 226–228.

Canfield, D.E., 1998. A new model for Proterozoic ocean chemistry. *Nature*, **396**, 450–453.

Canfield, D.E., Habicht, K.S. and Thamdrup, B., 2000. The Archean sulfur cycle and the early history of atmospheric oxygen. *Science*, **288**, 658–661.

Canfield, D.E. and Raiswell, R., 1999. The evolution of the sulfur cycle. *Am. J. Sci.*, **299**, 697–723.

Canfield, D.E. and Teske, A., 1996. Late Proterozoic rise in atmoispheric oxygen concentration inferred from phylogenetic and sulphur-isotope studies. *Nature*, **382**, 127–132.

Chumakov, N.M. and Elston, D.P., 1989. The paradox of Late Proterozoic glaciations at low latitudes. *Episodes*, **12**, 115–120.

Christie-Blick, N., Dyson, I.A. and von der Borch, C.C., 1995. Sequence stratigraphy and the interpretation of Neoproterozoic Earth history. *Precambrian Res.*, **73**, 3–26.

Christie-Blick, N., Sohl, L.E. and Kennedy, M.J., 1999. Considering a Neoproterozoic snowball Earth. *Science*, **284** online (http://www.sciencemag.org/cgi/content/full/284/5417/1087a).

Clauer, N., 1987. New information on the probable isotopic age of the late Proterozoic glaciation in West Africa. *Precambrian Res.*, **37**, 89–94.

Cloud, P.E., Wright, L.A., Williams, E.G., Diehl, P. and Walter, M.R., 1974. Giant stromatolites and associated vertical tubes from the Upper Proterozoic Noonday Dolomite, Death Valley region, eastern California. *Geol. Soc. Am. Bull.*, **85**, 1869–1882.

Colman, A.S. and Holland, H.D., 2000. The global diagenetic flux of phosphorus from marine sediments to the oceans: redox sensitivity and the control of atmospheric oxygen levels. In: *Marine Authigenesis: from Global to Microbial* (C. R. Glenn, L. Prévôt-Lucas and J. Lucas, eds). *Soc. Econ. Paleont. Mineral., Spec. Publ.*, **66**, 53–75.

Condon, D.J. and Prave, A.R., 2000. Two from Donegal: Neoproterozoic glacial episodes on the northeast margin of Laurentia. *Geology*, **28**, 951–954.

Condon, D.J., Prave, A.R. and Benn, D.I., 2002. Neoproterozoic glacial-rainout intervals: observations and implications. *Geology*, **30**, 35–38.

Corkeron, M.L. and George, A.D., 2001. Glacial incursion on a Neoproterozoic carbonate platform in the Kimberley region, Australia. *Geol. Soc. Am. Bull.*, **113**, 1121–1132.

Corsetti, F.A. and Kaufman, A.J., in press. Stratigraphic investigations of carbon isotope anomalies and Neoproterozoic ice ages in Death Valley, California. *Geol. Soc. Am. Bull.*, in press.

Crawford, A.R. and Daily, B., 1971. Probable non-synchroneity of Late Precambrian glaciations. *Nature*, **230**, 111–112.

Croll, J., 1867. On the excentricity of the earth's orbit, and its physical relations to the glacial epoch. *Phil. Mag.*, **33**, 119–131.

Crowell, J.C., 1983. Ice ages recorded on Gondwanan continents, Du Toit Memorial Lecture, 18. *Geol. Soc. S. Afr. Trans.*, **86**, 237–262.

Crowell, J.C., 1999. Pre-Mesozoic ice ages: their bearing on understanding the climate system. *Mem. Geol. Soc. Am.*, **192**.

Crowley, T.J., Hyde, W.T. and Peltier, W.R., 2001. CO_2 levels required for deglaciation of a 'near-snowball' Earth. *Geophys. Res. Lett.*, **28**, 283–286.

Crowley, T.J. and North, G.R., 1991. *Paleoclimatology*. Oxford University Press, New York.

Dalrymple, R.W. and Narbonne, G.M., 1996. Continental slope sedimentation in the Sheepbed Formation (Neoproterozoic, Windermere Supergroup), Mackenzie Mountains, N.W.T. *Can. J. Earth Sci.*, **33**, 848–862.

Dempster, T.J., Rogers, G., Tanner, P.W.G., Bluck, B.J., Muir, R.J., Redwood, S.D., Ireland, T.R. and Paterson, B.A., 2002. Timing of deposition, orogenesis and glaciation within the Dalradian rocks of Scotland: constraints from U–Pb zircon ages. *J. Geol. Soc., Lond.*, **159**, 83–94.

Derry, L.A., Kaufman, A.J. and Jacobsen, S.B., 1992. Sedimentary cycling and environmental change in the Late Proterozoic: evidence from stable and radiogenic isotopes. *Geochim. Cosmochim. Acta*, **56**, 1317–1329.

Des Marais, D.J. and Moore, J.G., 1984. Carbon and its isotopes in mid-oceanic basaltic glasses. *Earth Planet. Sci. Lett.*, **69**, 43–57.

Des Marais, D.J., Strauss, H., Summons, R.E. and Hayes, J.M., 1992. Carbon isotope evidence for the stepwise oxidation of the Proterozoic environement. *Nature*, **359**, 605–609.

Deynoux, M., 1980. Les Formations Glaciaires Du Précambriens Terminal et de la Fin de l'Ordovicien En Afrique de l'Ouest. *Travaux Des Laboratoires Des Sciences de la Terre St. Jérôme*, Marseille.

Deynoux, M., 1982. Periglacial polygonal structures and sand wedges in the Late Precambrian glacial formations of the Taoudeni Basin in Adrar of Mauretania (West Africa). *Palaeogeogr. Palaeoclimat. Palaeoecol.*, **39**, 55–70.

Deynoux, 1985. Terrestrial or waterlain glacial diamictites? Three case studies from the Late Precambrian and Late Ordovician glacial drifts in West Africa. *Palaeogeogr. Palaeoclimat. Palaeoecol.*, **51**, 97–141.

Deynoux, M., Kocurek, G. and Proust, J.N., 1989. Late Proterozoic periglacial aeolian deposits on the West African Platform, Taoudeni Basin, western Mali. *Sedimentology*, **36**, 531–549.

Deynoux, M. and Trompette, R., 1976. Late Precambrian mixtite: glacial and/or non-glacial? Dealing especially with the mixtite of West Africa. *Am. J. Sci.*, **276**, 117–125.

Drever, J.I., 1974. Geochemical model for the origin of Precambrian banded iron formations. *Geol. Soc. Am. Bull.*, **85**, 1099–1106.

Dunn, P.R., Thomson, B.P. and Rankama, K., 1971. Late Precambrian glaciation in Australia as a stratigiraphic boundary. *Nature*, **231**, 498–502.

Edwards, M.B., 1984. Sedimentology of the Upper Proterozoic glacial record, Verstertana Group, Finnmark, North Norway. *Nor. Geol. Unders. Bull.*, **394**.

Eisbacher, G.H., 1981. Sedimentary tectonics and glacial record in the Windermere Supergroup, Mackenzie Mountains, northwestern Canada. *Geol. Surv. Can. Pap.*, **80–27**.

Embleton, B.J.J. and Williams, G.E., 1986. Low palaeolatitude of deposition for late Precambrian periglacial varvites in South Australia: implications for paleoclimatology. *Earth Planet. Sci. Lett.*, **79**, 419–430.

Eriksson, E., 1968. Air–ocean–icecap interactions in relation to climatic fluctuations and glaciation cycles. *Meteor. Monogr.*, **8**, 68–92.

Evans, D.A.D., 2000. Stratigraphic, geochronological, and paleomagnetic constraints upon the Neoproterozoic climatic paradox. *Am. J. Sci.*, **300**, 347–433.

Evans, D.A., Beukes, N.J. and Kirschvink, J.L., 1997. Low-latitude glaciation in the Palaeoproterozoic era. *Nature*, **386**, 262–266.

Eyles, N., 1993. Earth's glacial record and its tectonic setting. *Earth-Sci. Rev.*, **35**, 1–248.

Fairchild, I.J., 1993. Balmy shores and icy wastes: the paradox of carbonates associated with glacial deposits in Neoproterozoic times. In: *Sedimentology Review 1* (V. P. Wright, ed.), pp. 1–16. Blackwell Scientific Publications, Oxford.

Fairchild, I.J. and Hambrey, M.J., 1984. The Vendian succession of northeastern Spitsbergen: petrogenesis of a dolomite–tillite association. *Precambrian Res.*, **26**, 111–167.

Farquhar, J., Bao, H. and Thiemens, M., 2000. Atmospheric influence of Earth's earliest sulfur cycle. *Science*, **289**, 756–758.

Fedonkin, M.A., 1992. Vendian faunas and the early evolution of metazoa. In: *Origin and Early Evolution of the Metazoa* (J. H. Lipps and P. W. Signor, eds), pp. 87–129. Plenum Press, New York.

Fedonkin, M.A., 1996. The oldest fossil animals in ecological perspective. In: *New Perspectives on the History of Life* (M. T. Ghiselin and G. Pinna, eds). *Mem. Calif. Acad. Sci.*, **20**, 31–45.

Fedonkin, M.A. and Waggoner, B.M., 1997. The Late Precambrian fossil Kimberella is a mollusc-like blaterian organism. *Nature*, **388**, 868–871.

Frimmel, H.E., Folling, P.G. and Eriksson, P.G., 2002. Neoproterozoic tectonic and climatic evolution recorded in the Gariep Belt, Namibia and South Africa. *Basin Res.*, **14**, 55–67.

Gaidos, E.J., Nealson, K.H. and Kirschvink, J.L., 1999. Life in ice-covered oceans. *Science*, **284**, 1631–1633.

German, T.N., 1990. *Organicheskii mir milliard let nazad (Organic World a Billion Years Ago)*. Nauka, St. Petersburg.

Gorokhov, I.M., Siedlecka, A., Roberts, D., Melnikov, N.N. and Turchenko, T.L., 2001. Rb–Sr dating of diagenetic illite in Neoproterozoic shales, Varanger Peninsula, northern Norway. *Geol. Mag.*, **138**, 541–562.

Graf, J.L., O'Connor, E.A. and van Leeuwen, P., 1994. Rare earth element evidence of origin and depositional environment of Late Proterozoic ironstone beds and manganese-oxide deposits, SW Brazil and SE Bolivia. *J. S. Am. Earth Sci.*, **7**, 115–133.

Grey, K., 1998. *Ediacarian acritarchs of Australia*. PhD Thesis, Macquarie University.

Grey, K. and Corkeron, M., 1998. Late Neoproterozoic stromatolites in glacigenic successions of the Kimberley region, Western Australia: evidence for a younger Marinoan glaciation. *Precambrian Res.*, **92**, 65–87.

Grotzinger, J.P. and James, N.P., 2000. Precambrian carbonates: evolution of understanding. In: *Carbonate Sedimentation and Diagenesis in the Evolving Precambrian World* (J. P. Grotzinger and N. P. James, eds). *SEPM Spec. Publ.*, **67**, 3–20.

Grotzinger, J.P. and Knoll, A.H., 1995. Anomalous carbonate precipitates: is the Precambrian the key to the Permian? *Palaios*, **10**, 578–596.

Halverson, G.P., Hoffman, P.F., Schrag, D.P. and Kaufman, A.J., 2002. A major perturbation of the carbon cycle before the Ghaub glaciation (Neoproterozoic) in Namibia: prelude to snowball Earth? *Geochem. Geophys. Geosystems*, in press.

Halverson, G.P. and Maloof, A.C., 2001. *Getting into global glaciation. J. Conference Abstract., 6, 104*. Eur. Un. Geosci., Strasbourg.

Hambrey, M.J. and Harland, W.B., 1981, *.Earth's Pre-Pleistocene Glacial Record*. Cambridge University Press, Cambridge.

Harland, W.B., 1964. Evidence of Late Precambrian glaciation and its significance. In: *Problems in Palaeoclimatology* (A. E. M. Nairn, ed.),pp. 119–149, 180–184. Interscience. John Wiley & Sons, London.

Harland, W.B., 1997. The Geology of Svalbard. *Geol. Soc. (London) Mem.*, **17**.

Harland, W.B. and Bidgood, D.E.T., 1959. Palaeomagnetism in some Norwegian sparagmites and the Late Pre-Cambrian ice age. *Nature*, **184**, 1860–1862.

Harland, W.B., Hambrey, M.J. and Waddams, P., 1993. Vendian geology of Svalbard. *Norsk Polarinstitut Skrifter*, **193**.

Harland, W.B. and Rudwick, M.J.S., 1964. The great infra-Cambrian ice age. *Sci. Am.*, **211**, 28–36.

Harland, W.B. and Wilson, C.B., 1956. The Hecla Hoek succession in Ny Friesland, Spitsbergen. *Geol. Mag.*, **93**, 265–286.

Hegenberger, W., 1987. Gas escape structures in Precambrian peritidal carbonate rocks. *Communs. Geol. Surv. S.W. Africa/Namibia*, **3**, 49–55.

Hegenberger, W., 1993. Stratigraphy and sedimentology of the Late Precambrian Witvlei and Nama Groups, east of Windhoek. *Geol. Surv. Namibia Mem.*, **17**.

Hoffmann, K.-H. and Prave, A.R., 1996. A preliminary note on a revised subdivision and regional correlation of the Otavi Group based on glaciogenic diamictites and associated cap dolostones. *Communs. Geol. Surv. Namibia*, **11**, 81–86.

Hoffman, P.F., Halverson, G.P. and Grotzinger, J.P., 2002a. Are Proterozoic cap carbonates and isotopic excursions a record of gas hydrate destabilization following Earth's coldest intervals? Comment. *Geology*, **30**, 286–287.

Hoffman, P.F., Halverson, G.P., Soffer, G., Schrag, D.P., Bowring, S.A. and DePaolo, D.J., 2001. Theme and variations on Neoproterozoic cap-carbonate sequences: signatures of snowball Earth events. *J. Conf Abstract., Eur. Un. Geosci.*, **6**, 99.

Hoffman, P.F., Kaufman, A.J. and Halverson, G.P., 1998a. Comings and goings of global glaciations on a Neoproterozoic tropical platform in Namibia. *GSA Today*, **8**, 1–9.

Hoffman, P.F., Kaufman, A.J., Halverson, G.P. and Schrag, D.P., 1998b. A Neoproterozoic snowball Earth. *Science*, **281**, 1342–1346.

Hoffman, P.F. and Maloof, A.C., 1999. Glaciation: the snowball theory still holds water. *Nature*, **397**, 384.

Hoffman, P.F. and Schrag, D.P., 1999. Response: Considering a Neoproterozoic snowball Earth. *Science*, **284** online (http://www.sciencemag.org/cgi/content/full/284/5417/1087a).

Hoffman, P.F., 1999. The break-up of Rodinia, birth of Gondwana, true polar wander and the snowball Earth. *J. Afr. Earth Sci.*, **28**, 17–33.

Hoffman, P.F. and Schrag, D.P., 2000. Snowball Earth. *Sci. Am.*, **282**, 62–75.

Hoffman, P.F., Van Dusen, A., Maloof, A.C., Ferguson, C. and Schrag, D.P., 2002b. Glimpse of a terrestrial snowball ocean: sea-floor dolomite-barite-aragonite sequence in a Neoproterozoic cap carbonate, northern Canadian Cordillera. Astrobiology Science Conference 2002. Abstract. NASA, Ames, California, in press.

Hofmann, H.J., Narbonne, G.M. and Aitken, J.D., 1990. Ediacaran remains from intertillite beds in northwestern Canada. *Geology*, **18**, 1199–1202.

Holland, H.D., 1984. *The Chemical Evolution of the Atmosphere and Oceans*. Princeton University Press, Princeton, NJ.

Hotinski, R.M., Bice, K.L., Kump, L.R., Najjar, R.G. and Arthur, M.A., 2001. Ocean stagnation and end-Permian anoxia. *Geology*, **29**, 7–10.

Howchin, W., 1908. Glacial beds of Cambrian age in South Australia. *Quat. J. Geol. Soc. Lond.*, **64**, 234–259.

Hunt, B.G., 1982. The impact of large variations of the Earth's obliquity on the climate. *J. Meteor. Soc. Jpn*, **60**, 309–318.

Hyde, W.T., Crowley, T.J., Baum, S.K. and Peltier, W.R., 2000. Neoproterozoic 'snowball Earth' simulations with a coupled climate/ice-sheet model. *Nature*, **405**, 425–429.

Ikeda, T. and Tajika, E., 1999. A study of the energy balance climate model with CO_2-dependent outgoing radiation: implication for the glaciation during the Cenozoic. *Geophys. Res. Lett.*, **26**, 349–352.

Isley, A.E. and Abbott, D.H., 1999. Plume-related mafic volcanism and the deposition of banded iron formation. *J. Geophys. Res.*, **104**, 15,461–15,415,477.

Ito, T., Masuda, K., Hamano, Y. and Matsui, T., 1995. Climate friction: a possible cause for secular drift of Earth's obliquity. *J. Geophys. Res.*, **100**, 15,147–15,161.

Jacobsen, S.B. and Kaufman, A.J., 1999. The Sr, C and O isotopic evolution of Neoproterozoic seawater. *Chem. Geol.*, **161**, 37–57.

James, N.P., Narbonne, G.M. and Kyser, T.K., 2001. Late Neoproterozoic cap carbonates: Mackenzie Mountains, northwestern Canada: precipitation and global glacial meltdown. *Can. J. Earth Sci.*, **38**, 1229–1262.

Jenkins, R.J.F., 1992. Functional and ecological aspects of Ediacaran assemblages. In: *Origin and Early Evolution of the Metazoa* (J. H. Lipps and P. W. Signor, eds), pp. 131–176. Plenum Press, New York.

Jenkins, G.S., 2000. Global climate model high-obliquity soluti8on to the ancient climate puzzles of the faint-young Sun paradox and low-latitude Proterozoic glaciation. *J. Geophys. Res.*, **105**, 7357–7370.

Jenkins, G.S. and Smith, S.R., 1999. GCM simulations of snowball Earth conditions during the late Proterozoic. *Geophys. Res. Lett.*, **26**, 2263–2266.

Kah, L.C., Lyons, T.W. and Chesley, J.T., 2001. Geochemistry of a 1.2 Ga carbonate-evaporite succession, northern Baffin and Bylot Islands: implications for Mesoproterozoic marine evolution. *Precambrian Res.*, **111**, 203–234.

Karhu, J.A. and Holland, H.D., 1996. Carbon isotobes and the rise of atmospheric oxygen. *Geology*, **24**, 149–152.

Kauffman, E.G., Arthur, M.A., Howe, B. and Scholle, P.A., 1996. Widespread venting of methane-rick fluids in Late Cretaceous (Campanian) submarine springs (Tepee Buttes), Western Interior seaway, U.S.A. *Geology*, **24**, 799–802.

Kaufman, A.J., Hayes, J.M., Knoll, A.H. and Germs, G.J.B., 1991. Isotopic compositions of carbonates and organic carbon from upper Proterozoic successions in Namibia: stratigraphic variation and the effects of diagenesis and metamorphism. *Precambrian Res.*, **49**, 301–327.

Kaufman, A.J. and Knoll, A.H., 1995. Neoproterozoic variations in the C-isotopic composition of seawater: stratigraphic and biogeochemical implications. *Precambrian Res.*, **73**, 27–49.

Kaufman, A.J., Knoll, A.H. and Narbonne, G.M., 1997. Isotopes, ice ages, and terminal Proterozoic earth history. *Proc. Natl. Acad. Sci. USA*, **94**, 6600–6605.

Kendall, C.G.St.C. and Warren, J., 1987. A review of the origin and setting of tepees and their associated fabrics. *Sedimentology*, **34**, 1007–1028.

Kennedy, M.J., 1996. Stratigraphy, sedimentology, and isotope geochemistry of Australian Neoproterozoic postglacial cap dolostones: deglaciation, $\delta^{13}C$ excursions, and carbonate precipitation. *J. Sed. Res.*, **66**, 1050–1064.

Kennedy, M.J., Christie-Blick, N. and Prave, A.R., 2001b. Carbon isotopic composition of Neoproterozoic glacial carbonates as a test of paleoceanographic models for snowball Earth phenomena. *Geology*, **29**, 1135–1138.

Kennedy, M.J., Christie-Blick, N. and Sohl, L.E., 2001a. Are Proterozoic cap carbonates and isotopic excursions a record of gas hydrate destabilization following Earth's coldest intervals. *Geology*, **29**, 443–446.

Kennedy, M.J., Runnegar, B., Prave, A.R., Hoffmann, K.-H. and Arthur, M.A., 1998. Two or four Neoproterozoic glaciations? *Geology*, **26**, 1059–1063.

Kent, D.V. and Smethurst, M.A., 1998. Shallow bias of paleomagnetic inclinations in the Paleozoic and Precambrian. *Earth Planet. Sci. Lett.*, **160**, 391–402.

Kirschvink, J.L., 1992. Late Proterozoic low-latitude global glaciation: the snowball earth. In: *The Proterozoic Biosphere* (J. W. Schopf and C. Klein, eds), pp. 51–52. Cambridge University Press, Cambridge.

Kirschvink, J.L., Gaidos, E.J., Bertani, L.E., Beukes, N.J., Gutzmer, J., Maepa, L.N. and Steinberger, R.E., 2000. Paleoproterozoic snowball Earth: extreme climatic and geochemical global change and its biological consequences. *Proc. Natl. Acad. Sci.*, **97**, 1400–1405.

Klein, C. and Beukes, N.J., 1993. Sedimentology and geochemistry of the glaciogenic late Proterozoic Rapitan iron-formation in Canada. *Econ. Geol.*, **84**, 1733–1774.

Knoll, A.H., 1994. Proterozoic and Early Cambrian protists: evidence for accelerating evolutionary tempo. *Proc. Natl. Acad. Sci. USA*, **91**, 6743–6750.

Knoll, A.H., 2000. Learning to tell Neoproterozoic time. *Precambrian Res.*, **100**, 3–20.

Knoll, A.H., Bambach, R.K., Canfield, D.E. and Grotzinger, J.P., 1996. Comparative Earth history and Late Permian mass extinction. *Science*, **273**, 452–457.

Knoll, A.H. and Carroll, S.B., 1999. Early animal evolution: emerging views from comparative biology and geology. *Science*, **284**, 2129–2137.

Knoll, A.H., Hayes, J.M., Kaufman, A.J., Swett, K. and Lambert, I.B., 1986. Secular variation in carbon isotope ratios from Upper Proterozoic successions of Svalbard and East Greenland. *Nature*, **321**, 832–838.

Knoll, A.H. and Walter, M.R., 1992. Latest Proterozoic stratigraphy and Earth history. *Nature*, **356**, 673–678.

Köppen, W. and Wegener, A., 1924, .*Die Klimate der Geologischen Vorzeit*. Gebrüder Borntraeger, Berlin.

Kröner, A., 1977. Non-synchroneity of Late Precambrian glaciations in Africa. *J. Geol.*, **85**, 289–300.

Kroopnick, P.M., 1985. The distribution of ^{13}C and $\sum CO_2$ in the world oceans. *Deep-Sea Res.*, **32**, 57–84.

Kump, L.R., 1991. Interpreting carbon-isotopic excursions: Strangelove oceans. *Geology*, **19**, 299–302.

Kump, L.R. and Arthur, M.A., 1999. Interpreting carbon-isotope excursions: carbonates and organic matter. *Chem. Geol.*, **161**, 181–198.

Kump, L.R. and Seyfried, W.E. Jr, 2001. Depressurization of hydrothermal vents during snowball Earth: effects on ocean chemistry. *Earth System Processes, Edinburgh, Scotland, Progr. Abstracts*, pp. 110, Geological Society, London.

Lachenbruch, A.H., 1962. Mechanics of thermal contraction cracks and ice-wedge polygons in permafrost. Geol. Soc. Am. Spec. Pap., 70.

Lasaga, A.C., 1998. *Kinetic Theory in the Earth Sciences*. Princeton University Press, Princeton.

Laskar, J., Joutel, F. and Robutel, P., 1993. Stabilization of the Earth's obliquity by the Moon. *Nature*, **361**, 615–617.

Lemke, P., 2001. Open windows to the polar oceans. *Science*, **292**, 1670–1671.

Lemon, N.M. and Gostin, V.A., 1990. Glacigenic sediments of the late Proterozoic Elatina Formation and equivalents, Adelaide Geosyncline, South Australia. In: *The Evolution of a Late Precambrian—Early Paleozoic Rift Complex: the Adelaide Geosyncline* (J. B. Jago and P. S. Moore, eds). *Geol. Soc. Aust. Spec. Publ.*, **16**, 149–163.

Leovy, C., 2001. Weather and climate on Mars. *Nature*, **412**, 245–249.

Li, Z.X., 2000. New palaeomagnetic results from the 'cap dolomite' of the Neoproterozoic Walsh tillite, northwestern Australia. *Precambrian Res.*, **100**, 359–370.

Logan, G.A., Hayes, J.M., Hieshima, G.B. and Summons, R.E., 1995. Terminal Proterozoic reorganization of biogeochemical cycles. *Nature*, **376**, 53–56.

Lottermoser, B.G. and Ashley, P.M., 2000. Geochemistry, petrology and origin of Neoproterozoic ironstones in the eastern part of the Adelaide geosyncline, South Australia. *Precambrian Res.*, **101**, 49–67.

MacAyeal, D.R., 1993. A low-order model of the Heinrich Event cycle. *Palaeoceanography*, **8**, 767–773.

Maloof, A.C., Kellogg, J.B. and Anders, A.M., 2002. On the origin of Neoproterozoic sand wedge polygons. *Astrobiology Science Conference* Abstract, NASA, Ames, CA, in press.

Manabe, S. and Broccoli, A.J., 1985. The influence of continental ice sheets on the climate of an ice age. *J. Geophys. Res.*, **90**, 2167–2190.

Marshall, H.G., Walker, J.C.G. and Kuhn, W.R., 1988. Long-term climate change and the geochemical cycle of carbon. *J. Geophys. Res.*, **93**, 791–801.

Martin, H., 1965. *The Precambrian geology of South West Africa and Namaqualand.* Precambrian Research Unit. University of Cape Town, South Africa.

Martin, M.W., Grazhdankin, D.V., Bowring, S.A., Evans, D.A.D., Fedonkin, M.A. and Kirschvink, J.L., 2000. Age of Neoproterozoic bilaterian body and trace fossils, White Sea, Russia: implications for metazoan evolution. *Science*, **288**, 841–845.

Maugh, T.H. 1989. Super ice age gave life on Earth growing pains. *Los Angeles Times*, September 7, pp. 1, 3, 28.

Mawson, D., 1949a. The late Precambrian ice-age and glacial record of the Bibliando dome. *J. Proc. Roy. Soc. New South Wales*, **82**, 150–174.

Mawson, D., 1949b. The Elatina glaciation. *Trans. R. Soc. S. Aust.*, **73**, 117–121.

McCabe, C. and Elmore, R.D., 1989. The occurrence and origin of late Paleozoic remagnetization in the sedimentary rocks of North America. *Rev. Geophys.*, **27**, 471–494.

McElhinny, M.W., Giddings, J.W. and Embleton, B.J.J., 1974. Palaeomagnetic results and late Precambrian glaciations. *Nature*, **248**, 557–561.

McElhinny, M.W. and McFadden, P.L., 2000, .*Paleomagnetism*. Academic Press, San Diego.

McKay, C.P., 2000. Thickness of tropical ice and photosynthesis on a snowball Earth. *Geophys. Res. Lett.*, **27**, 2153–2156.

McKirdy, D.M., Burgess, J.M. and Lemon, N.M., YuX., Cooper, A.M., Gostin, V.A., Jenkins, R.J.F. and Both, R.A., 2001. A chemostratigraphic overview of the late Cryogenian interglacial sequence in the Adelaide fold-thrust belt, South Australia. *Precambrian Res.*, **106**, 149–186.

McMechan, M.E., 2000. Vreeland diamictites—Neoproterozoic glaciogenic slope deposits, Rocky Mountains, northeast British Columbia. *Can. Bull. Petrol. Geol.*, **48**, 246–261.

McMillan, M.D., 1968. The geology of the Witputs-Sendelingsdrif area. *Bull. Precambr. Res. Unit*, **4**. University of Cape Town.

Miller, J.M.G., 1985. Glacial and syntectonic sedimentation: the upper Proterozoic Kingston Peak Formation, southern Panamint Range, eastern California. *Geol. Soc. Am. Bull.*, **96**, 1537–1553.

Moussine-Pouchkine, A. and Bertrand-Sarfati, J., 1997. Tectonosedimentary subdivisions in the Neoproterozoic to Early Cambrian cover of the Taoudeni Basin (Algeria-Mauritania-Mali). *J. Afr. Earth Sci.*, **24**, 425–443.

Murakami, T., Utsunomiya, S., Imazu, Y. and Prasad, N., 2001. Direct evidence of late Archean to early Proterozoic anoxic atmosphere from a product of 2.5 Ga old weathering. *Earth Planet. Sci. Lett.*, **184**, 523–528.

Myrow, P.M. and Kaufman, A.J., 1999. A newly discovered cap carbonate above Varanger-age glacial deposits in Newfoundland. *Can. J. Sed. Res.*, **69**, 784–793.

Narbonne, G.M., 1994. New Ediacaran fossils from the Mackenzie Mountains, northwestern Canada. *J. Paleont.*, **68**, 411–416.

Narbonne, G.M. and Aitken, J.D., 1990. Ediacaran fossils from the Sekwi Brook area, Mackenzie Mountains, northwestern Canada. *Palaeontology*, **33**, 945–980.

Narbonne, G.M. and Aitken, J.D., 1995. Neoproterozoic of the Mackenzie Mountains, northwestern Canada. *Precambrian Res.*, **73**, 101–121.

Néron de Surgy, O. and Laskar, J., 1997. On the long term evolution of the spin of the Earth. *Astron. Astrophys.*, **318**, 975–989.

Norin, E., 1937. *Geology of the western Quruq Tagh, eastern Tien Shan. Reports of the Sino-Swedish Expedition III. Geology*. Bokförlags Aktiebolaget Thule, Stockholm.

North, G.R., Cahalan, R.F. and Coakley, J.A., 1981. Energy balance climate models. *Rev. Geophys. Space Phys.*, **19**, 91–121.

Oglesby, R.J. and Ogg, J.G., 1999. The effect of large fluctuations in obliquity on climates of the late Proterozoic. *Paleoclimates*, **2**, 293–316.

Ojakangas, R.W., 1988. Glaciation: an uncommon 'mega-event' as a key to intracontinental and intercontinental correlation of Early Proterozoic basin fill, North American and Baltic cratons. In: *New Perspectives in Basin Analysis* (K. L. Kleinspehn and C. Paola, eds), pp. 431–444. Springer, New York.

Pais, M.A., Le Mouël, J.L., Lambeck, K. and Poirier, J.P., 1999. Late Precambrian paradoxical glaciation and obliquity of the Earth—a discussion of dynamical constraints. *Earth Planet. Sci. Lett.*, **174**, 155–171.

Park, J.K., 1997. Paleomagnetic evidence for low-latitude glaciation during deposition of the Neoproterozoic Rapitan Group, Mackenzie Mountains, N.W.T., Canada. *Can. J. Earth Sci.*, **34**, 34–49.

Pavlov, A.A., Kasting, J.F., Brown, L.L., Rages, K.A. and Freedman, R., 2000. Greenhouse warming by CH_4 in the atmosphere of early Earth. *J. Geophys. Res.*, **105**, 11,981–11,911,990.

Perry, W.J. and Roberts, H.G., 1968. Late Precambrian glaciated pavements in the Kimberley region, Western Australia. *J. Geol. Soc. Aust.*, **15**, 51–56.

Peryt, T.M., Hoppe, A., Bechstädt, T., Köster, J., Pierre, C. and Richter, D.K., 1990. Late Proterozoic aragonitic cement crusts, Bambuí Group, Minas Gerais, Brazil. *Sedimentology*, **37**, 279–286.

Peterson, K.J. and Takacs, C., 2001. Fossils, molecular clocks and the Cambrian explosion. *Geol. Soc. Am., Abstract. Progr.*, **33**, 430.

Plumb, K.A., 1981. Late Proterozoic (Adelaidean) tillites of the Kimberley–Victoria River region, Western Australia and Northern Territory. In: *Earth's Pre-Pleistocene Glacial Record* (M. J. Hambrey and W. B. Harland, eds), pp. 504–514. Cambridge University Press, Cambridge.

Pollard, D. and Kasting, J.K., 2001. Coupled GCM-ice sheet simulations of Sturtian (750–720 Ma) glaciation: When in the snowball-Earth cycle can tropical glaciation occur? *Eos*, **82**, S8.

Porter, S.M. and Knoll, A.H., 2000. Testate amoebae in the Neoproterozoic Era: evidence from vase-shaped microfossils in the Chuar Group, Grand Canyon. *Paleobiology*, **26**, 360–385.

Poulsen, C.J., Pierrehumbert, R.T. and Jacob, R.L., 2001. Impact of ocean dynamics on the simulation of the Neoproterozoic 'snowball Earth'. *Geophys. Res. Lett.*, **28**, 1575–1578.

Powell, C.McA., Pisarevsky, S.A. and Wingate, M.T.D., 2001. An animated history of Rodinia. *Geol. Soc. Aus., Abstract.*, **65**, 85–87.

Prasad, N. and Roscoe, S.M., 1996. Evidence for anoxic to oxic atmospheric change during 2.45–2.22 Ga from lower and upper sub-Huronian paleosols. *Catena*, **27**, 105–121.

Prave, A.R., 1999a. Two diamictites, two cap carbonates, two $\delta^{13}C$ excursions, two rifts: the Neoproterozoic Kingston Peak Formation, Death Valley, California. *Geology*, **27**, 339–342.

Prave, A.R., 1999b. The Neoproterozoic Dalradian Supergroup of Scotland: an alternative hypothesis. *Geol. Mag.*, **136**, 609–617.

Preiss, W.V., 1987. The Adelaide Geosyncline. *S. Aust. Department Mines Energ. Bull.*, **53**.

Priscu, J.C., Fritsen, C.H., Adams, E.E., Giovanni, S.J., Paerl, H.W., McKay, C.P., Doran, P.T., Gordon, D.A., Lanoil, B.D. and Pinckney, J.L., 1998. Perennial Antarctic lake ice: an oasis for life in a polar desert. *Science*, **280**, 2095–2098.

Reusch, H., 1891. Skuringsmærker og morængrus eftervist i Finnmarken fra en periode meget ældre end 'istiden'. *Norges Geol. Unders.*, **1**, 78–85 (97–100 English summary).

Rice, A.H.N. and Hofmann, C.-C., 2000. Evidence for a glacial origin of Neoproterozoic III striations at Oaibaccannjar'ga, Finnland, northern Norway. *Geol. Mag.*, **137**, 355–366.

Roberts, J.D., 1976. Late Precambrian dolomites, Vendian glaciation, and synchroneity of Vendian glaciations. *J. Geol.*, **84**, 47–63.

Runnegar, B., 1982. The Cambrian explosion: animals or fossils? *J. Geol. Soc. Aust.*, **29**, 395–411.

Runnegar, B., 2000. Loophole for snowball Earth. *Nature*, **405**, 403–404.

Rye, R. and Holland, H.D., 1998. Paleosols and the evolution of atmospheric oxygen: a critical review. *Am. J. Sci.*, **298**, 621–672.

Saltzman, M.R., Ripperdan, R.L., Brasier, M.D., Lohman, K.C., Robison, R.A., Chang, W.T., Peng, S., Ergaliev, E.K. and Runnegar, B., 2000. A global carbon isotope excursion (SPICE) during the Late Cambrian: relation to trilobite extinctions, organic-matter burial and sea level. *Palaeogeogr. Palaeoclimat. Palaeoecol.*, **162**, 211–223.

Saylor, B.Z., Kaufman, A.J., Grotzinger, J.P. and Urban, F., 1998. A composite reference section for terminal Proterozoic strata of southern Namibia. *J. Sediment. Res.*, **68**, 1223–1235.

Schermerhorn, L.J.G., 1974. Late Precambrian mixtites: glacial and/or non-glacial? *Am. J. Sci.*, **274**, 673–824.

Schermerhorn, L.J.G. and Stanton, W.I., 1963. Tilloids in the West Congo geosyncline. *Quart. J. Geol. Soc. Lond.*, **119**, 201–241.

Schmidt, P.W. and Williams, G.E., 1995. The Neoproterozoic climatic paradox: equatorial paleolatitude for Marinoan glaciation near sea level in South Australia. *Earth Planet. Sci. Lett.*, **134**, 107–124.

Schmidt, P.W. and Williams, G.E., 1999. Paleomagnetism of the Paleoproterozoic hematitic breccia and paleosol at Ville-Marie, Québec: further evidence for the low paleolatitude of Huronian glaciation. *Earth Planet. Sci. Lett.*, **172**, 273–285.

Schmidt, P.W., Williams, G.E. and Embleton, B.J.J., 1991. Low palaeolatitude of Late Proterozoic glaciation: early timing of remanence in haematite of the Elatina Formation, South Australia. *Earth Planet. Sci. Lett.*, **105**, 355–367.

Schopf, J.W., 1991. Collapse of the Late Proterozoic ecosystem. *S. Afr. J. Geol.*, **94**, 33–43.

Schrag, D.P., Berner, R.A. and Hoffman, P.F., 2002. On the initiation of a snowball Earth. *Geochem. Geophys. Geosystems*, in press.

Schrag, D.P. and Hoffman, P.F., 2001. Life, geology and snowball Earth. *Nature*, **409**, 306.

Seilacher, A., 1992. Vendobionta and Psammocorallia: lost constructions of Precambrian evolution. *J. Geol. Soc., Lond.*, **149**, 607–613.

Sellers, W.D., 1969. A global climatic model based on the energy balance of the Earth-atmosphere system. *J. Appl. Meteor.*, **8**, 392–400.

Sheldon, R.P., 1984. Ice-ring origin of the Earth's atmosphere and hydrosphere and Late Proterozoic–Cambrian phosphogenesis. *Geol. Surv. India. Spec. Publ.*, **17**, 17–21.

Shields, G., Stille, P., Brasier, M.D. and Atudorei, N.-V. 1997. Stratified oceans and oxygenation of the late Precambrian environment: a post glacial geochemical record from the Neoproterozoic of W. Mongolia. *Terra Nova*, **9**, 218–222.

Soffer, G., 1998. *Evolution of a Neoproterozoic continental margin subject to tropical glaciation.* B.A. Thesis, Harvard College, Cambridge, MA.

Sohl, L.E., Christie-Blick, N. and Kent, D.V., 1999. Paleomagnetic polarity reversals in Marinoan (ca. 600 Ma) glacial deposits of Australia: implications for the duration of low-latitude glaciations in Neoproterozoic time. *Geol. Soc. Am. Bull.*, **111**, 1120–1139.

Spencer, A.M., 1971. Late Pre-Cambrian glaciation in Scotland. *Mem. Geol. Soc. Lond.*, **6**.

Spencer, A.M. and Spencer, M.O., 1972. The Late Precambrian/Lower Cambrian Bonahaven Dolomite of Islay and its stromatolites. *Scott. J. Geol.*, **8**, 269–282.

Sprigg, R.C., 1947. Early Cambrian (?) jellyfishes from the Flinders Ranges, South Australia. *Trans. R. Soc. S. Aust.*, **71**, 212–224.

Sprigg, R.C., 1952. Sedimentation in the Adelaide geosyncline and the formation of the continental terrace. In: *Sir Douglas Mawson Anniversary Volume* (M. F. Glaessner and E. A. Rudd, eds), pp. 153–159. University of Adelaide, Adelaide.

Sprigg, R.C., 1990. The Adelaide Geosyncline: a century of controversy. In: *The Evolution of a Late Precambrian—Early Paleozoic Rift Complex: the Adelaide Geosyncline* (J. B. Jago and P. S. Moore, eds). *Geol. Soc. Aust. Spec. Publ.*, **16**, 66–83.

Summons, R.E. and Hayes, J.M., 1992. Principles of molecular and isotopic biogeochemistry. In: *The Proterozoic Biosphere, a Multidisciplinary Study* (J. W. Schopf and C. Klein, eds), pp. 83–93. Cambridge University Press, Cambridge.

Sumner, D.Y., in press. Rapid calcite and aragonite precipitation in late Archean carbonates and Neoproterozoic cap carbonates. In: *Precambrian Sedimentary Environments* (W. Altermann, ed.). *Spec. Publ. Int. Ass. Sed.*

Sumner, D.Y. and Grotzinger, J.P., 1996. Were kinetics of Archean calcium carbonate precipitation related to oxygen concentration? *Geology*, **24**, 119–122.

Sumner, D.Y., Kirschvink, J.L. and Runnegar, B.N., 1987. Soft-sediment paleomagnetic fold tests of late Precambrian glaciogenic sediments. *Eos*, **68**, 1251.

Thomas, D.N. and Dieckmann, G.S., 2002. Antarctic sea ice—a habitat for extremophiles. *Science*, **295**, 641–644.

Thompson, M.D. and Bowring, S.A., 2000. Age of the Squantum 'tillite', Boston basin, Masschusetts: U-Pb zircon constraints on terminal Neoproterozoic glaciation. *Am. J. Sci.*, **300**, 630–655.

Torsvik, T.H., Smethurst, M.A., Meert, J.G., Van der Voo, R., McKeroow, W.S., Brasier, M.D., Sturt, B.A. and Walderhaug, H.J., 1996. Continental break-up and collision in the Neoproterozoic and Palaeozoic—a tale of Baltica and Laurentia. *Earth Sci. Rev.*, **40**, 229–258.

Trompette, R., de Alvarenga, C.J.S. and Walde, D., 1998. Geological evolution of the Neoproterozoic Corumbá graben system (Brazil): depositional context of the stratified Fe and Mn ores of the Jacadigo Group. *J. S. Am. Earth Sci.*, **11**, 587–597.

Tsikos, H. and Moore, J.M., 1998. The Kalahari manganese field: an enigmatic association of iron and manganese. *S. Afr. J. Geol.*, **101**, 287–290.

Urban, H., Stribrny, B. and Lippolt, H.J., 1992. Iron and manganese deposits of the Urucum district, Mato Grosso do Sul, Brazil. *Econ. Geol.*, **87**, 1375–1392.

Van Cappellen, P. and Ingall, E.D., 1994. Benthic phosphorus regeneration, net primary production, and ocean anoxia: a model of the coupled marine biogeochemical cycles of carbon and phosphorus. *Paleoceanography*, **9**, 677–692.

Van Wagoner, J.C., Posamentier, H.W., Mitchum, R.M., Vail, P.R., Sarg, J.F., Loutit, T.S. and Hardenbol, J., 1988. An overview of the fundamentals of sequence stratigraphy and key definitions. In: *Sea-Levels Changes—an Integrated Approach* (C. K. Wilgus, H. Posamenier, C. A. Ross and C. G. St. C. Kendall, eds). *Soc. Econ. Paleont. Mineral. Spec. Publ.*, **42**, 39–45.

Veizer, J., Ala, D., Azmy, K., Bruckschen, P., Buhl, D., Bruhn, F., Carden, G.A.F., Diener, A., Ebneth, S., Godderis, Y., Jasper, T., Korte, C., Pawellek, F., Podlaha, O.G. and Strauss, H., 1999. $^{87}Sr/^{86}Sr$, $\delta^{13}C$ and $\delta^{18}O$ evolution of Phanerozoic seawater. *Chem. Geol.*, **161**, 59–88.

Veizer, J., Clayton, R.N. and Hinton, R.W., 1992. Geochemistry of Precambrian carbonates. IV. Early Paleoproterozoic (2.25 ± 0.25 Ga) seawater. *Geochim. Cosmochim. Acta*, **56**, 875–885.

Vidal, G. and Knoll, A.H., 1982. Radiations and extinctions of plankton in the late Proterozoic and early Cambrian. *Nature*, **297**, 57–60.

Vidal, G. and Moczydlowska-Vidal, M., 1997. Biodiversity, speciation, and extinction trends of Proterozoic and Cambrian phytoplankton. *Paleobiology*, **23**, 230–246.

Vincent, W.F. and Howard-Williams, C., 2000. Life on snowball Earth. *Science*, **287**, 2421.

von der Borch, C.C., Christie-Blick, N. and Grady, A.E., 1988. Depositional sequence analysis applied to Late Proterozoic Wilpena Group, Adelaide Geosyncline, South Australia. *Aust. J. Earth Sci.*, **35**, 59–71.

Walker, J.C.G., 2001. Strange weather on snowball Earth. *Earth System Processes, Edinburgh, Scotland, Progr. Abstracts*, pp. 110–111, Geological Society, London.

Walker, J.C.G. and Brimblecombe, P., 1985. Iron and sulfur in the pre-biologic ocean. *Precambrian Res.*, **28**, 205–222.

Walker, J.C.G., Hays, P.B. and Kasting, J.F., 1981. A negative feedback mechanism for the long-term stabilization of Earth's surface temperature. *J. Geophys. Res.*, **86**, 9776–9782.

Walker, J.C.G., 2001. Strange weather on snowball Earth. *Earth System Processes, Edinburgh, Scotland, Progr. Abstracts*, pp. 110–111, Geological Society, London.

Walter, M.R. and Bauld, J., 1983. The association of sulphate evaporites, stromatolitic carbonates and glacial sediments: examples from the Proterozoic of Australia and the Cainozoic of Antarctica. *Precambrian Res.*, **21**, 63–81.

Walter, M.R., Veevers, J.J., Calver, C.R., Gorjan, P. and Hill, A.C., 2000. Dating the 840–544 Ma Neoproterozoic interval by isotopes of strontium, carbon, and sulfur in seawater, and some interpretive models. *Precambrian Res.*, **100**, 371–433.

Wang, Y., Lu, S., Gao, Z., Lin, W. and Ma, G., 1981. Sinian tillites of China. In: *Earth's Pre-Pleistocene Glacial Record* (M. J. Hambrey and W. B. Harland, eds), pp. 386–401. Cambridge University Press, Cambridge.

Warren, S.G., Brandt, R.E., Grenfell, T.C. and McKay, C.P., 2002. Snowball Earth: ice thickness on the tropical ocean. *J. Geophys. Res. (Oceans)*, in press.

Wegener, A., 1922. *The Origin of Continents and Oceans*, 3rd edn (J.G.A. Skerl, transl.). Methuen, London.

Wetherald, R.T. and Manabe, S., 1975. The effects of changing the solar constant on the climate of a general circulation model. *J. Atmos. Sci.*, **32**, 2044–2059.

Williams, G.E., 1975. Late Precambrian glacial climate and the Earth's obliquity. *Geol. Mag.*, **112**, 441–444.

Williams, G.E., 1979. Sedimentology, stable-isotope geochemistry and palaeoenvironment of dolostones capping late Precambrian glacial sequences in Australia. *J. Geol. Soc. Australia*, **26**, 377–386.

Williams, G.E., 1993. History of the Earth's obliquity. *Earth-Sci. Rev.*, **34**, 1–45.

Williams, G.E., 1996. Soft-sediment deformation structures from the Marinoan glacial succession, Adelaide foldbelt: implications for the paleolatitude of late Neoproterozoic glaciation. *Sediment. Geol.*, **106**, 165–175.

Williams, G.E., 1998. Late Neoproterozoic periglacial aeolian sand sheet, Stuart Shelf, South Australia. *Aust. J. Earth Sci.*, **45**, 733–741.

Williams, G.E., 2000. Geological constraints on the Precambrian history of the Earth's rotation and the Moon's orbit. *Rev. Geophys.*, **38**, 37–59.

Williams, D.M., Kasting, J.F. and Frakes, L.A., 1998. Low-latitude glaciation and rapid changes in the Earth's obliquity explained by obliquity-oblateness feedback. *Nature*, **396**, 453–455.

Williams, G.E. and Schmidt, P.W., 1997. Paleomagnetism of the Proterozoic Gowganda and Lorrain formations, Ontario: low paleolatitude for Huronian glaciation. *Earth Planet. Sci. Lett.*, **153**, 157–169.

Williams, G.E. and Schmidt, P., 2000. Proterozoic equatorial glaciation: Has 'snowball Earth' a snowball's chance? *The Aust. Geologist*, **117**, 21–25.

Williams, G.E. and Tonkin, D.G., 1985. Periglacial structures and paleoclimatic significance of a late Precambrian block field in the Cattle Grid copper mine, Mount Gunson, South Australia. *Aust. J. Earth Sci.*, **32**, 287–300.

Worsley, T.R. and Kidder, D.L., 1991. First-order coupling of paleogeography and CO_2 with global surface temperature and its latitudinal contrast. *Geology*, **19**, 1161–1164.

Wright, L., Williams, E.G. and Cloud, P., 1978. Algal and cryptalgal structures and platform environments of the late pre-Phanerozoic Noonday Dolomite, eastern California. *Geol. Soc. Am. Bull.*, **89**, 321–333.

Xiao, S., Yuan, X., Kaufman, A.J., Bao, H. and Wang, H., 2001. Neoproterozoic diamictites and stable carbon isotope chemostratigraphy of the Quruqtagh series, NW China. *Geol. Soc. Am. Abstract. Progr.*, **33**, A-144.

Yeo, G.M., 1981. The late Proterozoic Rapitan glaciation in the northern Cordillera. In: *Proterozoic Basins of Canada* (F.H.A. Campbell, ed.). *Geol. Surv. Can. Pap.*, **81–10**.

Yeo, G.M., 1986. Iron-formation in the late Proterozoic Rapitan Group, Yukon and Northwest Territories. In: *Mineral Deposits of Northern Cordillera* (J.A. Morin, ed.), *Can. Inst. Mining Metallurgy Spec. Vol.*, **37**, 142–153.

Young, G.M., 1973. Tillites and aluminous quartzites as possible time markers for middle Precambrian (Aphebian) rocks of North America. In: *Huronian Stratigraphy and Sedimentation* (G. M. Young, ed.). *Geol. Assoc. Can. Spec. Pap.*, **12**, 97–125.

Young, G.M., 1976. Iron-formation and glaciogenic rocks of the Rapitan Group, Northwest Territories, Canada. *Precambrian Res.*, **3**, 137–158.

Young, G.M., 1988. Proterozoic plate tectonics, glaciation and iron-formations. *Sediment. Geol.*, **58**, 127–144.

Young, G.M., 1995. Are Neoproterozoic glacial deposits preserved on the margins of Laurentia related to the fragmentation of two supercontinents? *Geology*, **23**, 153–156.

Young, G.M. and Gostin, V.A., 1991. Late Proterozoic (Sturtian) succession of the North Flinders basin, South Australia: and example of temperate glaciation in an active rift setting. In: *Glacial Marine Sedimentation: Paleoclimatic Significance* (J. B. Anderson and G. M. Ashley, eds). *Geol. Soc. Am. Spec. Pap.*, **261**, 207–222.

Zhang, Y., Yin, L., Xiao, S., and Knoll, A.H., 1988. Permineralized fossils from the terminal Proterozoic Doushantuo Formation, South China. *Paleont. Soc. Mem.*, **50**, 1–52.

Zhang, R., Follows, M.J., Grotzinger, J.P. and Marshall, J., 2001. Could the Late Permian deep ocean have been anoxic? *Paleoceanography*, **16**, 317–329.

Received 31 January 2002; accepted 12 February 2002

